การสังเคราะห์เชื้อเพลิงดีเซลโดยตรงจากปฏิกิริยาฟิชเชอร์โทรป

โดย

บรรเจิด จงสมจิตร

สถาบันวิทยบริการ
จุฬาลงกรณ์มหาวิทยาลัย

คณะวิศวกรรมศาสตร์
จุฬาลงกรณ์มหาวิทยาลัย
กรุงเทพฯ
มกราคม 2548

สถาบันวิทยบริการ
จุฬาลงกรณ์มหาวิทยาลัย

การสังเคราะห์เชื้อเพลิงดีเซลโดยตรงจากปฏิกิริยาฟิชเชอร์โทรป

โดย

บรรเจิด จงสมจิตร Ph.D. (Pittsburgh)

สถาบันวิทยบริการ
จุฬาลงกรณ์มหาวิทยาลัย

คณะวิศวกรรมศาสตร์

จุฬาลงกรณ์มหาวิทยาลัย

กรุงเทพฯ

มกราคม 2548

สารบัญ

สถาบันวิทยบริการ
จุฬาลงกรณ์มหาวิทยาลัย

แบบรายงานความก้าวหน้าของการวิจัยที่ได้รับการสนับสนุน

ยุทธศาสตร์การพัฒนาศักยภาพการแข่งขันอุตสาหกรรม กลุ่ม Basic and Strategic Industry

โครงการวิจัยเรื่อง (ภาษาไทย)   การสังเคราะห์เชื้อเพลิงดีเซลโดยตรงจากปฏิกิริยาฟิชเชอร์โทรป

          (ภาษาอังกฤษ)   Direct Synthesis of Diesel Fuel from Fischer-Tropsch Reaction

ได้รับทุนอุดหนุนการวิจัยประจำปีงบประมาณ 2547 จำนวนเงิน 952,600 บาท

รายงานความก้าวหน้าของการวิจัยของการวิจัย 1 ปี เริ่มทำการวิจัยเมื่อ ตุลาคม 2546

รายงานความก้าวหน้าของการวิจัย ครั้งที่ 2 ระหว่าง ตุลาคม 2546 ถึง กันยายน 2547

รายนามคณะผู้วิจัย พร้อมทั้งหน่วยงานที่สังกัดและหมายเลขโทรศัพท์

ลำดับ	ชื่อ-นามสกุล	หน้าที่	หน่วยงานที่สังกัด	โทรศัพท์ (โทรสาร)
1	นายบรรเจิด จงสมจิตร	ผู้วิจัยหลัก	คณะวิศวกรรมศาสตร์ จุฬาฯ	2186869 (2186877)
2	นางจูงใจ ปั้นประณด	ผู้วิจัยร่วม	คณะวิศวกรรมศาสตร์ จุฬาฯ	2186859 (2186877)

ลงชื่อ ....

(นายบรรเจิด จงสมจิตร)

ผู้วิจัยหลัก

30 กันยายน 2547

หัวข้อรายละเอียดเกี่ยวกับผลงานความก้าวหน้าของการวิจัยที่ส่งมาด้วย

1. วัตถุประสงค์ของโครงการ

2. สรุปตารางเปรียบเทียบระหว่างแผนงานวิจัยที่เสนอไว้ในโครงการกับงานวิจัยที่ได้ดำเนินการไปแล้ว

3. รายละเอียดของผลงานวิจัยที่ได้ดำเนินการไปแล้ว

4. งานตามโครงการที่จะทำในงวดที่ 3

5. บทความวิจัยที่ได้รับการตีพิมพ์ในวารสารระดับนานาชาติในงานวิจัยนี้จำนวน 1 บทความ
   (Catalysis Letters (ISI): Impact factor 1.852)

บทนำ

เชื้อเพลิงดีเซล (C_{10}-C_{20}) เป็นผลิตภัณฑ์ที่ได้จากการกลั่นน้ำมันดิบในช่วงอุณหภูมิระหว่าง 160-300°C ผลิตภัณฑ์ที่ได้สามารถนำไปใช้เป็นเชื้อเพลิงของเครื่องยนต์ดีเซล นอกจากวิธีดังกล่าวแล้วการสังเคราะห์เชื้อเพลิงดีเซลยังสามารถทำได้โดยใช้ปฏิกิริยาฟิชเชอร์-โทรป (Fischer-Tropsch Synthesis หรือ FTS) ซึ่งเป็นปฏิกิริยาโพลีเมอร์ไรเซชันของไฮโดรเจนและคาร์บอนมอนอกไซด์หรือแก๊สสังเคราะห์ (Syngas) ที่ได้จากปฏิกิริยา Steam reforming ของแก๊สธรรมชาติ หรือการเผาไหม้ของถ่านหิน ซึ่งแสดงได้ในรูปที่ 1 เชื้อเพลิงดีเซลที่ได้จากปฏิกิริยา FTS จะมีความบริสุทธิ์สูง ไม่เป็นพิษต่อสิ่งแวดล้อมเนื่องจากไม่มีสารปนเปื้อน เช่น ซัลเฟอร์ ซึ่งพบในเชื้อเพลิงดีเซลที่ได้จากน้ำมันดิบ
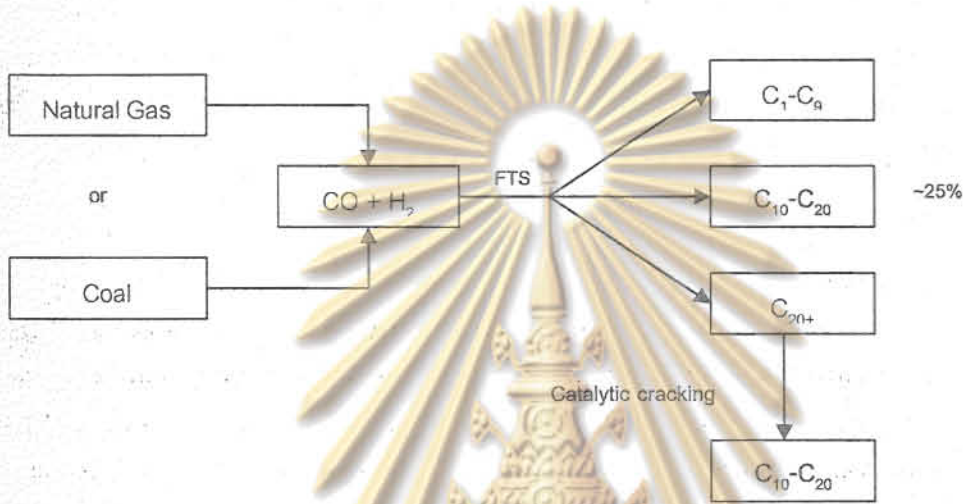
รูปที่ 1 แสดงการสังเคราะห์เชื้อเพลิงดีเซล (C_{10}-C_{20}) จากปฏิกิริยา FTS และ catalytic cracking

อย่างไรก็ตามจากการวิจัยในอดีตพบว่าสัดส่วนที่สามารถผลิตได้มากที่สุดของเชื้อเพลิงดีเซลจากปฏิกิริยา FTS มีอัตราส่วนประมาณ 25% ของผลิตภัณฑ์ทั้งหมด ผลิตภัณฑ์ส่วนใหญ่ที่ได้จาก FTS จะอยู่ในรูปของ wax (C_{20+}) ซึ่งต้องนำไปทำปฏิกิริยาในขั้นต่อไป คือ Catalytic Cracking เพื่อให้ได้ผลิตภัณฑ์ที่มีค่าสูงขึ้นเช่นน้ำมันเบนซินและน้ำมันดีเซล ต่อไป การเกิดผลิตภัณฑ์เป็นไฮโดรคาร์บอนหลายชนิด (C_1-C_{20+}) ในปฏิกิริยา Fischer-Tropsch synthesis นี้เป็นข้อจำกัดที่ไม่สามารถเปลี่ยนแปลงได้ เนื่องจาก การเติบโตของสายโซ่ไฮโดรคาร์บอน (hydrocarbon chain growth) ถูกควบคุมโดยหลักการทางจลนพลศาสตร์ของพอลีเมอไรเซชั่น หลักการดังกล่าวมีชื่อเรียกว่า Anderson-Schulz-Flory (ASF) kinetics ตามชื่อของผู้ค้นพบ โดยทั่วไปกลไกการเกิดปฏิกิริยาของ Fischer-Tropsch synthesis ประกอบด้วยการแตกตัวของไฮโดรเจนและการแตกตัวของคาร์บอนมอนออกไซด์ในขณะที่มีการดูดซับบนตัวเร่งปฏิกิริยา (dissociative adsorption) เป็น surface species (C* และ H*) ซึ่งจะเกิดเป็นไฮโดรคาร์บอนต่อไปโดยการพอลีเมอไรเซชั่น โดยที่ Hydrogenated surface carbon species (CH*) จะทำหน้าที่เป็นมอโนเมอร์สำหรับการเติบโตของไฮโดรคาร์บอนต่อไป (CH* + CH* → C_2H_2*) ดังนั้นผลิตภัณฑ์ที่ได้จากปฏิกิริยา Fischer-Tropsch synthesis จึงประกอบด้วยไฮโดรคาร์บอนที่มีเลขคาร์บอน (carbon number) หลากหลาย(C_1-C_{20+}) ทั้งนี้ อัตราส่วนที่มากที่สุดของของผลิตภัณฑ์ที่สามารถสังเคราะห์ได้จากปฏิกิริยา FTS โดยการเปลี่ยนแปลงสภาวะที่ใช้ในการทำปฏิกิริยา คือ มีเทน 100%, C_2-C_4 โอเลฟิน 56%, แก๊สโซลีน 48%, เชื้อเพลิงดีเซล 25% และ wax 80% [1] อย่างไรก็ตามได้มีการ

ค้นคว้าวิจัยเพื่อเปลี่ยนแปลงสัดส่วนของผลิตภัณฑ์จากปฏิกิริยา FTS โดยวิธีการต่างๆ ซึ่งสามารถสรุป
ได้พอสังเขปดังนี้

1. การใช้ตัวเร่งปฏิกิริยาที่มีซีโอไลท์เป็นองค์ประกอบ [2-24]

ในช่วงปี 1980-2000 งานวิจัยที่เกี่ยวข้องกับปฏิกิริยา FTS ได้มุ่งเน้นไปทางด้านการเพิ่มผลผลิต
เชื้อเพลิงเบนซิน (gasoline) มีการนำเอาซีโอไลท์มาใช้เป็นส่วนประกอบในตัวเร่งปฏิกิริยา งานวิจัย
บางส่วนได้รายงานความสำเร็จในการเพิ่มผลิตภัณฑ์ในช่วง C_5-C_9 โดยผู้วิจัยดังกล่าวได้เสนอว่า
ไฮโดรคาร์บอนที่มีขนาดไม่เกิน C_9 เท่านั้นที่สามารถผ่านเข้าไปทำปฏิกิริยาในซีโอไลท์ได้ อย่างไรก็ตาม
ต่อมาได้มีการค้นพบว่าความเป็นกรดของพื้นผิวของซีโอไลท์มีบทบาทอย่างมากต่อการหยุดการเติบโต
ของสายโซ่ไฮโดรคาร์บอน Vanhove ได้แสดงว่าไฮโดรคาร์บอนสามารถกลั่นตัว (condense) ภายในรู
พรุนขนาดเล็กของซีโอไลท์จากนั้นจะเกิดปฏิกิริยา Hydrocracking เป็นไฮโดรคาร์บอนที่มีขนาดเล็กลง
โดยที่จุดที่มีความเป็นกรดบนซีโอไลท์มีความว่องไวในปฏิกิริยาชนิดนี้ โดยหลักฐานที่แสดงการค้นพบดัง
กล่าวคือการเกิดเป็นผลิตภัณฑ์ไอโซเมอร์ของไฮโดรคาร์บอนโซ่ตรง ซึ่งจะเกิดบนตำแหน่ง acid sites
ของซีโอไลท์เท่านั้น

2. การใช้เครื่องปฏิกรณ์แบบ 2 ขั้น (dual reactor) [25-27]

การใช้เครื่องปฏิกรณ์แบบ 2 ขั้นได้ถูกนำมาใช้เพื่อเพิ่มผลิตภัณฑ์แก๊สโซลีน โดยผลิตภัณฑ์ wax ที่
ได้จากปฏิกิริยา FTS ในขั้นแรกจะถูกส่งต่อไปยังเครื่องปฏิกรณ์ที่สอง (catalytic cracking reactor) ที่มีซี
โอไลท์ชนิด HZSM-5 เป็นตัวเร่งปฏิกิริยา เพื่อย่อยสลายเป็นผลิตภัณฑ์แก๊สโซลีนต่อไป อย่างไรก็ตาม
ระบบดังกล่าวไม่เป็นที่นิยมเนื่องจากต้นทุนการผลิตยังสูงกว่าการกลั่นน้ำมันจากน้ำมันดิบอยู่มาก

ในปัจจุบัน แนวโน้มของ Fischer-Tropsch synthesis ได้มุ่งเน้นการสังเคราะห์น้ำมันดีเซล
คุณภาพสูงจากก๊าซธรรมชาติ เนื่องจากมีการค้นพบแหล่งก๊าซธรรมชาติในพื้นที่ห่างไกลที่ยังไม่ถูก
นำมาใช้ประโยชน์หลายแห่งบนโลก ดังนั้นการสังเคราะห์ตัวเร่งปฏิกิริยาที่สามารถเพิ่มผลผลิตของ
เชื้อเพลิงดีเซลได้มากกว่า 25% จะเป็นประโยชน์อย่างมากในเชิงพาณิชย์ ทั้งนี้ข้อจำกัดของสารประกอบซี
โอไลท์คือ รูพรุนมีขนาดเล็ก จัดอยู่ในกลุ่ม microporous ซึ่งมีรูพรุนขนาดเส้นผ่าศูนย์กลางเล็กกว่า 2 นา
โนเมตร ซึ่งทำให้ขนาดของโมเลกุลที่จะผ่านเข้าไปเกิดปฏิกิริยาในซีโอไลท์อยู่ในช่วงแคบ เมื่อไม่นานมานี้
molecular sieves ชนิดที่มีรูพรุนขนาดกลาง หรือ mesoporous ได้ถูกสังเคราะห์ขึ้นโดย กลุ่มนักวิจัยของ
บ.โมบิลออยล์ ประเทศสหรัฐอเมริกา [28-30] ซึ่งได้เรียกกลุ่มสารชนิดนี้ว่า M41S โดยมี MCM-41 ซึ่ง
เป็นหนึ่งในสารกลุ่มนี้ที่ได้รับความสนใจจากนักวิจัยต่าง ๆ ค่อนข้างสูง MCM-41มีคุณลักษณะ คือ มี
พื้นที่ผิวสูง (โดยเฉลี่ยประมาณ 1,000 ตารางเมตรต่อกรัม) มีรูพรุนที่มีขนาดสม่ำเสมอ ขนาดเส้นผ่าน
ศูนย์กลางสังเคราะห์ได้ในช่วง 2-10 นาโนเมตรขึ้นอยู่กับสภาวะและวิธีการสังเคราะห์ มีความทนทานต่อ
สภาวะความร้อน (thermal) และความร้อนชื้น (hydrothermal) ที่สูง มีคุณสมบัติการดูดซับสูง รูปที่ 2
แสดงภาพการสังเคราะห์ MCM-41 งานวิจัยที่เกี่ยวข้องกับการสังเคราะห์และศึกษาคุณลักษณะของ
MCM-41 สามารถค้นคว้าได้อย่างกว้างขวาง แต่ในอีกด้านหนึ่งงานวิจัยเชิงปฏิบัติในการนำ MCM-41 มา
ประยุกต์ใช้กับตัวเร่งปฏิกิริยา Fischer-Tropsch ยังไม่เป็นที่แพร่หลาย ทั้งนี้ตัวเร่งปฏิกิริยาที่มี MCM-41
เป็นส่วนประกอบมีความเป็นไปได้ที่จะยับยั้งการเติบโตของสายโซ่ไฮโดรคาร์บอนที่ขนาดของ
ไฮโดรคาร์บอนที่ใหญ่กว่าผลิตภัณฑ์ที่ได้จากการใช้ซีโอไลท์ ทำให้ได้ผลิตภัณฑ์ที่อยู่ในช่วงของเชื้อเพลิง
ดีเซลที่มากขึ้น
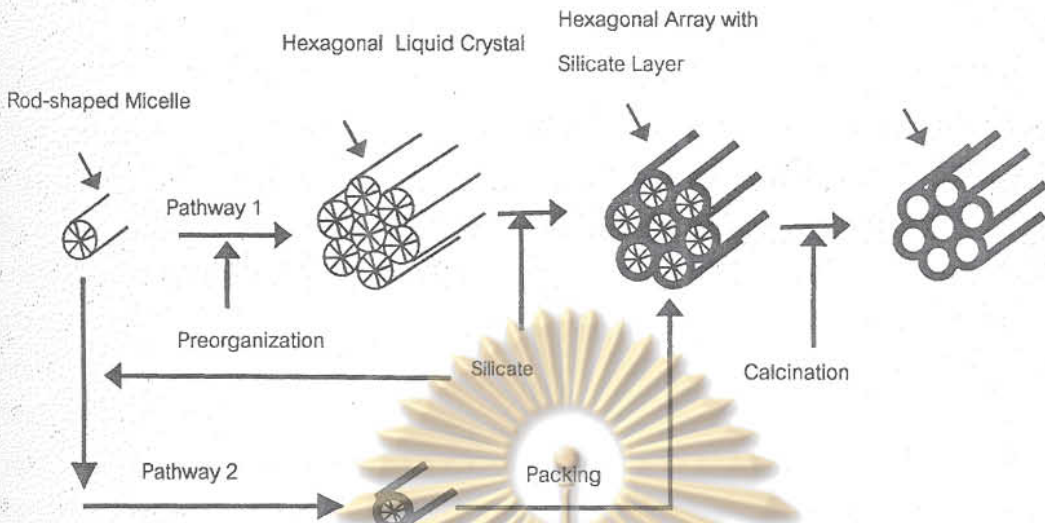
รูปที่ 2 แสดงภาพการสังเคราะห์ MCM-41

3. งานวิจัยที่เกี่ยวข้องกับตัวเร่งปฏิกิริยาฟิชเชอร์-โทรปที่มี MCM-41 เป็นองค์ประกอบ

ในปี 2002 Panpranot และคณะ [31-32] ได้รายงานการสังเคราะห์ตัวเร่งปฏิกิริยาโคบอลต์บนตัว
รองรับแบบ MCM-41 โดยมีรูเทเนียมเป็นตัวสนับสนุน (promoter) พบว่ามีอัตราการเกิดปฏิกิริยาสูงกว่า
ตัวเร่งปฏิกิริยาแบบดั้งเดิมที่มี ซิลิกาเจลเป็นตัวรองรับ อย่างไรก็ตามงานวิจัยดังกล่าวพบว่าการกระจาย
ตัวของโลหะโคบอลต์ไม่สม่ำเสมอบนตัวรองรับ MCM-41 เมื่อใช้สารประกอบโคบอลต์ในเตรทเป็นสารตั้ง
ต้นในการเตรียมตัวเร่งปฏิกิริยาจึงควรมีการขยายขอบเขตการศึกษาเพื่อสังเคราะห์ตัวเร่งปฏิกิริยา
โคบอลต์บนตัวรองรับแบบ MCM-41ที่มีการกระจายตัวของโคบอลต์สูงและมีประสิทธิภาพสูงต่อไป

**4.งานวิจัยที่เกี่ยวข้องกับผลกระทบของตัวรองรับต่อประสิทธิภาพของตัวเร่งปฏิกิริยาในปฏิกิริยาฟิช
เซอร์-โทรป**

โดยทั่วไปสมบัติทางเคมี (chemical property) ลักษณะของพื้นผิว (texture) และ ความเป็นกรดของ
พื้นผิว (surface acidity) ของตัวรองรับแต่ละชนิดจะมีผลต่อการกระจายตัวของโลหะ คุณสมบัติในการรี
ดิวซ์และปฏิกิริยาระหว่างโลหะและตัวรองรับ (metal-support interaction) Ruel และ Bartholomew [33]
รายงานว่าความว่องไวของตัวเร่งปฏิกิริยา 10% Co เพิ่มขึ้นตามลำดับดังนี้ $Co/MgO < Co/C < Co/SiO_2$
$< Co/Al_2O_3 < CoTiO_2$ นอกจากนี้ในงานวิจัยของ Vanhove [34] พบว่าค่าการเติบโตของสายโซ่
ไฮโดรคาร์บอนมีความสัมพันธ์กับขนาดของรูพรุนของตัวรองรับ ในงานวิจัยของ Iglesia [35-37] รายงาน
ว่าค่าการเลือกเกิดของ C_{5+} ที่แตกต่างกันเนื่องมาจากผลของสมบัติทางกายภาพและเคมีของตัวรองรับที่
แตกต่างกันโดยทำให้เกิดการดูดซับของสารมัธยันต์ (intermediates) บนพื้นผิวของตัวเร่งปฏิกิริยาที่แตก
ต่างกัน อย่างไรก็ตามตัวรองรับที่มีขนาดของรูพรุนอยู่ในช่วงกว้าง (wide pore size distribution) อาทิ
เช่น อะลูมินา ซิลิกา ไททาเนีย และเซอร์โคเนีย มักทำให้เกิดผลิตภัณฑ์ไฮโดรคาร์บอนที่หลากหลาย การ

ใช้สารที่มีขนาดของรูพรุนแคบ (narrow pore size distribution)มีผลต่อค่าการเลือกเกิดของผลิตภัณฑ์ต่างๆในปฏิกิริยาฟิชเชอร์โทรป

ประโยชน์ที่คาดว่าจะได้รับ

การเพิ่มผลผลิตของเชื้อเพลิงดีเซลที่ได้โดยตรงจากปฏิกิริยา FTS เป็นการลดต้นทุนการผลิตเนื่องจากเป็นการลดขั้นตอนในปฏิกิริยาการแยกสลายของ wax เพื่อให้ได้เชื้อเพลิงดีเซลซึ่งเป็นปฏิกิริยาต่อเนื่องจากปฏิกิริยา FTS อีกทางหนึ่ง เชื้อเพลิงดีเซลที่ได้จะมีความบริสุทธิ์สูงไม่เป็นพิษต่อสิ่งแวดล้อม เนื่องจากไม่มีสารตกค้างเจือปนเหมือนกับเชื้อเพลิงดีเซลที่ได้จากการ กลั่นน้ำมันดิบงานวิจัยดังกล่าวสามารถก่อให้เกิดการพัฒนาระบบของตัวเร่งปฏิกิริยาแบบใหม่ (Robust Catalysts) ที่สามารถจำกัดการเติบโตของสายโซ่ไฮโดรคาร์บอน (Limitation of Hydrocarbon Chain Growth) อีกด้วย ซึ่งแนวทางดังกล่าวอาจนำไปประยุกต์ใช้ได้กับปฏิกิริยาอื่น ๆ ที่ต้องการจำกัดการเกิดปฏิกิริยาเฉพาะผลิตภัณฑ์ตัวใดตัวหนึ่งที่ต้องการ (Desired Product) โดยไม่เกิดปฏิกิริยาต่อเนื่องไปเป็นผลิตภัณฑ์ที่ไม่ต้องการ (Undesired Product) ตัวอย่างของปฏิกิริยาดังกล่าวได้แก่ ปฏิกิริยาออกซิเดชันเพียงบางส่วน (Partial Oxidation of Methane) ของมีเทน เพื่อจำกัดปฏิกิริยาไว้เพียงเมทานอลหรือฟอร์มาลดีไฮด์โดยไม่เกิดปฏิกิริยาต่อเนื่องไปเป็นคาร์บอนไดออกไซด์เป็นต้น

ทฤษฎี สมมติฐานหรือกรอบแนวความคิด (Conceptual Framework) ของโครงการวิจัย

โลหะโคบอลด์บนตัวรองรับ (Supported Cobalt Catalysts) เป็นตัวเร่งปฏิกิริยาที่มีประสิทธิภาพอย่างสูงในการทำปฏิกิริยาสังเคราะห์แบบฟิชเชอร์โทรป เนื่องจากมีความว่องไว (Activity) สูง และให้อัตราส่วนของผลิตภัณฑ์ไฮโดรคาร์บอนที่มีสายโซ่ยาวสูงซึ่งอยู่ในรูปของ Wax (C_{20+}) ซึ่ง wax ที่ได้จะถูกนำไปทำการย่อยสลายได้ผลิตภัณฑ์ที่มีขนาดโมเลกุลเล็กลง ได้แก่ แก๊สโซลีนและเชื้อเพลิงดีเซลต่อไป อย่างไรก็ตามจากกระบวนการผลิตในปัจจุบันจะเห็นว่าการผลิตเชื้อเพลิงดีเซลให้เพียงพอไม่สามารถทำได้โดยใช้กระบวนการสังเคราะห์แบบฟิชเชอร์โทรปเพียงอย่างเดียว จำเป็นที่จะต้องนำ Wax ไปย่อยสลายอีกขั้นหนึ่งทำให้เสียค่าใช้จ่ายในส่วนดังกล่าว จากเหตุผลนี้เองทำให้เกิดแนวความคิดที่ว่าทำอย่างไรจึงจะสามารถเพิ่มผลผลิตของเชื้อเพลิงดีเซลในขั้นตอนการสังเคราะห์แบบฟิชเชอร์โทรปได้ ซึ่งปัจจุบันจะทำได้เพียง 25% ของผลิตภัณฑ์ทั้งหมดที่เกิดขึ้นเท่านั้น ที่เหลือก็จะได้ Wax เป็นส่วนใหญ่

จากการที่การสังเคราะห์แบบฟิชเชอร์โทรปจะมีพื้นฐานมาจากการปฏิกิริยาโพลิเมอร์ไรเซชันของหมู่เมทิลีน (CH_2-) ซึ่งเป็นผลของปฏิกิริยาการเติมไฮโดรเจนเข้าที่คาร์บอนมอนอกไซด์ (CO Hydrogenation) ทำให้เกิดเป็นสายโซ่ที่มีความยาวของสารประกอบไฮโดรคาร์บอนที่มีความยาวเพิ่มขึ้นตามดีกรีของปฏิกิริยาโพลิเมอร์ไรเซชันที่เพิ่มขึ้น ผลิตภัณฑ์ที่ได้ขึ้นอยู่กับปัจจัยหลายประการเช่นองค์ประกอบของตัวเร่งปฏิกิริยาที่ใช้การกระตุ้นตัวเร่งก่อนทำปฏิกิริยา และสภาวะของปฏิกิริยา เป็นต้น จากปัญหาที่พบคือ การเกิดเชื้อเพลิงดีเซลที่มีจำนวนคาร์บอนตั้งแต่ 10 – 20 อะตอม นั้น มีอัตราส่วนที่ต่ำ เนื่องจากการดำเนินไปของปฏิกิริยาโพลิเมอร์ไรเซชันยังคงมีอยู่ทำให้ได้สายโซ่ไฮโดรคาร์บอนที่มีความยาวมากขึ้น ทำอย่างไรจึงหยุดปฏิกิริยาไว้เพียงการเกิดเชื้อเพลิงดีเซลเท่านั้น ซึ่งทำให้เกิดแนวความคิดที่เรียกว่า การจำกัดการเติบโตของสายโซ่ไฮโดรคาร์บอน (Limitation of Hydrocarbon Chain Growth)

โครงการวิจัยที่นำเสนอนี้เป็นการหาแนวทางหรือกลยุทธ์ (Strategy) ในการจำกัดการเติบโตของสายโซ่ไฮโดรคาร์บอนไว้เพียงเชื้อเพลิงดีเซลเท่านั้นซึ่งอาจสามารถทำได้โดยการเปลี่ยนองค์ประกอบของตัวเร่งปฏิกิริยาที่มีองค์ประกอบที่เหมาะสม โดยเฉพาะการใช้ตัวรองรับที่เหมาะสมอาจทำให้การจำกัดการเติบโตของสายโซ่เป็นไปได้ง่ายขึ้น จากการที่ในปัจจุบันได้มีการสังเคราะห์ตัวรองรับต่าง ๆ ที่มีรูพรุนขนาดปานกลาง

(Mesoporous Materials) ซึ่งมีขนาดของรูพรุนอยู่ระหว่าง 1.5 –10 นาโนเมตร ซึ่งขนาดความกว้างของรูพรุน
นี้เองอาจเป็นตัวแปรสำคัญในการกลั่นกรองขนาดของโมเลกุล (Molecular Sieve) ที่ต้องการซึ่งจะเป็นการ
จำกัดขนาดของโมเลกุลที่ถูกดูดซับและคายออกมาเป็นผลิตภัณฑ์ที่ต้องการต่อไป นอกจากองค์ประกอบของ
ตัวเร่งปฏิกิริยาแล้ว สภาวะของปฏิกิริยา เช่น อุณหภูมิ ความดัน และเวลา ก็มีความสำคัญต่อการอัตราส่วน
ของผลิตภัณฑ์ที่เกิดขึ้นอีกด้วย อย่างไรก็ตามงานวิจัยนี้มุ่งเน้นการพัฒนาตัวเร่งปฏิกิริยาที่เหมาะสมสำหรับ
ปฏิกิริยาดังกล่าวเป็นหลัก

สถาบันวิทยบริการ
จุฬาลงกรณ์มหาวิทยาลัย

รายละเอียดเกี่ยวกับผลงานความก้าวหน้าของการวิจัย

(1) วัตถุประสงค์ของโครงการ

เป็นการศึกษาวิจัยพื้นฐานในการพัฒนาตัวเร่งปฏิกิริยาและกระบวนการสำหรับการผลิตน้ำมันดีเซล
ที่มีกำมะถันต่ำจากปฏิกิริยาฟิชเชอร์-โทรปให้มีประสิทธิภาพสูงกว่า 25%

สถาบันวิทยบริการ
จุฬาลงกรณ์มหาวิทยาลัย

รายละเอียดเกี่ยวกับผลงานความก้าวหน้าของการวิจัย

(2) สรุปตารางเปรียบเทียบระหว่างแผนงานวิจัยที่เสนอไว้ในโครงการกับงานวิจัยที่ได้ดำเนินการไปแล้ว

(2.1) ในรอบ 6 เดือน

กิจกรรม/ขั้นตอนการดำเนินงาน	ไตรมาส 1	ไตรมาส 2	ไตรมาส 3	ไตรมาส 4	ไตรมาส 5	ไตรมาส 6	ไตรมาส 7	ไตรมาส 8
ศึกษาค้นคว้าเอกสารเพิ่มเติม								
เตรียมอุปกรณ์และสารเคมี								
สังเคราะห์ MCM-41								
สังเคราะห์ Co/MCM-41								
สังเคราะห์ Co/SiO$_2$, Co/Al$_2$O$_3$								
สังเคราะห์ Co/TiO$_2$								

▨ แผนงานวิจัยที่เสนอไว้ในโครงการ

▨ งานวิจัยที่ทำได้จริง

สถาบันวิทยบริการ
จุฬาลงกรณ์มหาวิทยาลัย

9

(2.2) ในรอบ 1 ปี

กิจกรรม/ขั้นตอนการดำเนินงาน	ไตรมาส 1	ไตรมาส 2	ไตรมาส 3	ไตรมาส 4	ไตรมาส 5	ไตรมาส 6	ไตรมาส 7	ไตรมาส 8
ตรวจสอบลักษณะของตัวเร่ง			▓					
สร้าง FTS Reaction System			▓					
ตรวจวัด Activity/selectivity			▓	▓				
สรุปผลและทำรายงาน เพิ่มประสิทธิภาพของตัวเร่งปฏิกิริยา				▓				
สังเคราะห์ตัวเร่งปฏิกิริยา Co with promoters					▓			
ตรวจสอบลักษณะของตัวเร่ง						▓		
ตรวจวัด Activity/selectivity						▓		
ศึกษาผลของการเติมรูไทล์ เฟสลงใน Co/TiO$_2$						▓		
ตรวจสอบลักษณะของตัวเร่ง							▓	
ตรวจวัด Activity/selectivity							▓	
สรุปผลและจัดทำรายงาน								▓

▓ แผนงานวิจัยที่เสนอไว้ในโครงการ

▓ งานวิจัยที่ทำได้จริง

รายละเอียดเกี่ยวกับผลงานความก้าวหน้าที่ได้ดำเนินการไปแล้ว

(3) รายละเอียดของผลงานวิจัยที่ได้ดำเนินการไปแล้ว

(3.1) ในช่วง 6 เดือนแรกของปีที่ 1 ผลงานวิจัยที่ได้ดำเนินการไปแล้ว มีดังนี้

1. ค้นคว้าหาข้อมูลในการวิจัยเพื่อเตรียมตัวรองรับและตัวเร่งปฏิกิริยาจากวารสารต่างประเทศ
2. เตรียมอุปกรณ์และสั่งซื้อสารเคมีเพื่อใช้เตรียมตัวรองรับและตัวเร่งปฏิกิริยา
3. เตรียมตัวรองรับ MCM-41
4. สังเคราะห์ตัวเร่งปฏิกิริยาโคบอลต์บนตัวรองรับ ได้แก่ Co/MCM-41, Co/SiO$_2$, และ Co/TiO$_2$ โดยวิธี incipient impregnation method [13]

(3.2) ในช่วง 1 ปีแรก ผลงานวิจัยที่ได้ดำเนินการไปแล้วมีดังนี้

1. ตรวจสอบลักษณะ (Characterization) ของตัวเร่งปฏิกิริยาที่เตรียมได้
2. สร้าง FTS Reaction System เพื่อใช้ในการทดสอบความ Activity/selectivity ของตัวเร่งปฏิกิริยาที่เตรียมได้
3. ตรวจวัด Activity/selectivity ของตัวเร่งปฏิกิริยา
4. ตีพิมพ์บทความในวารสารต่างประเทศ (ตามเอกสารแนบ)
5. สรุปผลและจัดทำรายงานความก้าวหน้าครั้งที่ 2

สถาบันวิทยบริการ
จุฬาลงกรณ์มหาวิทยาลัย

สถาบันวิทยบริการ
จุฬาลงกรณ์มหาวิทยาลัย

รายการ	จำนวนเงินที่ได้รับ (บาท)	จำนวนเงินที่ใช้ไป (บาท)	จำนวนเงินที่เหลือ (บาท)
หมวดค่าจ้างชั่วคราว			
ค่าจ้างผู้ช่วยนักวิจัย 2 คน (อัตราเงินเดือน 6,360 บาท/เดือน)	152,640	152,640	-
หมวดค่าใช้สอย			
-ค่าจ้างเหมาพิมพ์รายงานและจัดทำราย งาน	7,700	6,721.50	978.50
-ค่าไปรษณีย์ต่างประเทศ	10,000	2,379	7,621
-ค่าจ้างวิเคราะห์ตัวอย่าง	200,000	114,703	85,297
หมวดค่าตอบแทน	95,260	-	95,260
หมวดค่าวัสดุ			
-ค่าจ้างทำเตาปฏิกรณ์	37,000	3,370.50	33,629.50
-ค่าวัสดุสำหรับประกอบเครื่องปฏิกรณ์	200,000	331,256.09	(131,256.09)
-ค่าสารเคมี	150,000	84,754.70	65,245.30
-ค่าแก็ส	50,000	85,107.80	(35,107.80)
-ค่าวัสดุสิ้นเปลือง	50,000	76,902.25	(26,902.25)
รวมทั้งสิ้น	952,600	857,834.84	94,765.16

สถาบันวิทยบริการ
จุฬาลงกรณ์มหาวิทยาลัย

เอกสารอ้างอิง (References)

1. Anderson, J.R., Structure of Metallic Catalysts, Academic Press, New York, (1975).
2. Bessell, S., U.S. Patent, 5,16,377 (1992).
3. Bessell, S., Appl. Catal., 96, 253 (1993).
4. Bessell, S., Stud. Surf. Sci. Catal. 81, 461 (1994).
5. Besell, S., Appl. Catal., 126, 235 (1995).
6. Caesar, P.D., Brennan, J.A., Garwood, W.E., and Ciric, J., J. Catal., 56, 274 (1979).
7. Calleja, G., Lucas, A.D., and Grieken, R.V., Appl. Catal., 11, 68 (1991).
8. Chang, C.D., Lang, W.H., and Silvestri, A.J., J. Catal., 56, 258 (1979).
9. Dry, M.E., Ander, J.R., and Boudart, M., In Catalysis-Science and Technology, Springer-Verlag, New York (1981).
10. Gormley, R.J., Rao, U.V.S., Anderson, R.R., Schehl, R.R., and Chi, R.D.H., J. Catal., 113, 195 (1988).
11. Hagg, W.O., and Huang, T.J., U.S. Patent, 4,279,830 (1981).
12. Koh, D.J., Chung, J.S., Kim, Y.G., Ind. Eng. Chem. Res., 34, 1969 (1995).
13. Iglesia, E., J. Catal., 153,188 (1995).
14. Stencel, J.M., Rao, V.U.S., Diehl, J.R., Rhee, K.H., Dhere, A.G., and DeAngelis, R.J., J. Catal., 84, 109 (1983).
15. Verma, R.L., and Jothimugesan, K., Can. J. Chem. Eng., 4, 141 (1986).
16. Chen, Y.W., Wang, H.T., and Goodwin, J.G., Jr., J. Catal., 83, 415 (1983).
17. Chen, Y.W., Wang, H.T., Goodwin, J.G., Jr. and Shiflett, W.K., Appl. Catal., 8, 303 (1983).
18. Chen, Y.W., Wang, H.T., and Goodwin, J.G., Jr., J. Catal., 85, 409 (1984).
19. Wang, H.T., Chen, Y.W., and Goodwin, J.G., Jr., Zeolites, 4, 56 (1984).
20. Oukaci, R., and Goodwin, J.G., Jr., Preprints of Fuel Chemistry Division (ACS),Anaheim, CA, Sep. 7-12 (1986).
21. Oukaci, R., Sayari, A., and Goodwin, J.G., Jr., J. Catal., 102, 126 (1986).
22. Oukaci, R. Sayari, A., and Goodwin, J.G., Jr., J. Catal., 106, 318 (1987).
23. Oukaci, R., Wu, J.C.S., and Goodwin, J.G., Jr., J. Catal., 107, 471 (1987).
24. Oukaci, R., Wu, J.C.S., and Goodwin, J.G., Jr., J. Catal., 110, 47 (1988).
25. Ohtsuka, K., Chem. Mater., 9, 2039 (1997).

26. Hagg, W.O., and Huang, T.J., U.S. Patent, 4,279,830 (1981).

27. Kuo, J.C.W., Final Report, DOE Contract DE-AC22-83PC60019 (1985).

28. Beck, J.C., Chu, C., Johnson, Z.D.,Kresge, C.T., Leonowicz, M.E., Roth, W.J., and Vartuli, J.C., World Patent W091/11390 (1991).

29. Beck, J.S., Vartuli, J.C., Roth, W.J.,Leonowicz, M.E., Kresge, C.T., Schmitt, K.D., Chu, C.T.W., Olson, D.H., Sheppard, E.W., McCullen, S.B., Higgins, J.B., and Schlenker, J.L., J. Am. Chem. Soc., 114 10834 (1992).

30. Kresge, C.T.,Leonowicz, M.E., Roth, W.J., Vartuli, J.C., and Beck, J.S., Nature, 359, 710 (1992).

31. Panpranot J., Goodwin, J. G., Jr., and Sayari A. Catal. Today 77, 269 (2002).

32. Panpranot J., Goodwin, J. G., Jr., and Sayari A. J. Catal. 211, 530 (2002).

33. Reuel R. C., Bartholomew C. H., J. Catal. 85, 78 (1984).

34. Vanhove D., Zhang Z., Makambo L., Blamchard M., App. Catal. 9, 327 (1984).

35. Iglesia E., App. Catal. A 161, 50 (1997)

36. Iglesia E., Soled S. L., Fiato R. A., J. Catal. 137, 212 (1992)

37. Iglesia E., Soled S. L., Fiato R. A., J. Catal. 143, 345 (1993)

สถาบันวิทยบริการ
จุฬาลงกรณ์มหาวิทยาลัย

<u>สรุปผลการดำเนินงานวิจัยตลอดระยะเวลา 1 ปี (Executive summary)</u>

ในระยะเวลา 1 ปีที่ผ่านมาการดำเนินงานวิจัยในหัวข้อดังกล่าวเป็นไปตามแผนที่วางไว้ และในบางส่วนก็มีความก้าวหน้ามากกว่าแผนที่วางไว้เช่นกัน โดยเฉพาะการมีบทความที่ได้รับการตีพิมพ์ในวารสารระดับนานาชาติซึ่งมี impact factor ถึง 1.581 (Catalysis Letters) ในระบบ Institute of Science Information (ISI) ถึง 2 เรื่อง อีกทั้งยังได้ผลิตมหาบัณฑิตที่มีคุณภาพอีกถึงสองคน ประจำปีการศึกษา 2547 คือ นางสาวจิตรลดา ศักดิ์ดามพ์นุสนธิ์ และนางสาวสุจารี แก้วกัน ทั้งนี้ยังรวมถึงงานวิจัยบางส่วนที่กำลังอยู่ในระหว่างการพิจารณา (in reviews) โดยผู้ทรงคุณวุฒิต่างประเทศอีกจำนวน 2 ฉบับ อย่างไรก็ตามงานวิจัยดังกล่าวถือว่าเป็นเพียงจุดเริ่มต้นของโครงการวิจัยนี้เท่านั้น การดำเนินการวิจัยเพื่อให้บรรลุวัตถุประสงค์ที่วางไว้นั้น มีความจำเป็นอย่างยิ่งที่จะต้องศึกษาในเชิงลึกซึ่งมีความจำเป็นอย่างยิ่งที่จะต้องใช้เครื่องมือวิเคราะห์และอุปกรณ์ที่ดีกว่าเครื่องมือที่มีอยู่ในปัจจุบัน ซึ่งก็ถือเป็นความโชคดีอีกเช่นกันที่เครื่องมือและครุภัณฑ์ภายใต้โครงการ OECF จะเข้ามาในช่วงปลายปีนี้ ทำให้การทำงานวิจัยในเรื่องนี้สามารถดำเนินการไปได้อย่างมีประสิทธิภาพ โดยเฉพาะเครื่องมือที่จำเป็นอย่างยิ่งสำหรับงานวิจัยนี้ ได้แก่ gas chromatography, X-ray photoelectron spectroscopy (XPS), chemisorption, temperature program reduction/oxidation และอื่น ๆ ดังนั้นในช่วงเวลาอีก 1 ปีที่เหลืออยู่ประสิทธิภาพในการทำวิจัยจะเพิ่มขึ้นและบรรลุวัตถุประสงค์ตามที่วางไว้

บทความวิจัยที่ได้รับการตีพิมพ์ในวารสารระดับนานาชาติ จำนวน 2 บทความ คือ

1. Joongjai Panprnot, Sujaree Kaewkun, Piyasan Praserthdam, and James G. Goodwin, Jr., *"Effect of cobalt precursors on the dispersion of cobalt on MCM-41"*. *Catalysis Letters*, 91 (2003), pp. 95-102. Impact factor =1.581 (ISI database)

2. Bunjerd Jongsomjit, Chitlada Sakdamnuson, James G. Goodwin, Jr., and Piyasan Praserthdam, *"Co-support compound formation in titania-supported cobalt catalyst"*, *Catalysis Letters*, 94 (2004), pp. 209-215. Impact factor = 1.581 (ISI database)

บทความวิจัยที่ส่งไปเพื่อตีพิมพ์และอยู่ในระหว่างการพิจารณา (in reviews) จำนวน 2 บทความ คือ

1. Bunjerd Jongsomjit, Chitlada Sakdamnuson, and Piyasan Praserthdam, *"Dependence of crytalline phases in titania on catalytic properties during CO hydrogenation of Co/TiO$_2$ catalysts"*, submitted to Materials Chemistry and Physics on July 10, 2004.

2. Joongjai Panpranot, Sujaree Kaewgun, and Piyasan Praserthdam, *"Metal-support interaction in mesoporous silica-supported cobalt Fischer-Tropsch catalysts"*, submitted to Reaction kinetics and catalysis letters on September 10, 2004.

International Publication
จำนวน 2 ฉบับ

สถาบันวิทยบริการ
จุฬาลงกรณ์มหาวิทยาลัย

Effect of cobalt precursors on the dispersion of cobalt on MCM-41

Joongjai Panpranot[a,*], Sujaree Kaewkun[a], Piyasan Praserthdam[a], and James G. Goodwin, Jr.[b]

[a]*Center of Excellence on Catalysis and Catalytic Reaction Engineering, Department of Chemical Engineering, Chulalongkorn University, Bangkok, 10330 Thailand*
[b]*Department of Chemical Engineering, Clemson University, South Carolina, 29634 USA*

Co/MCM-41 catalysts were prepared using the incipient wetness impregnation technique with aqueous solutions of different cobalt compounds such as cobalt nitrate, cobalt chloride, cobalt acetate, and cobalt acetylacetonate. MCM-41 is known to have a restricted pore structure; however, using organic precursors such as cobalt acetate and cobalt acetylacetonate resulted in very small cobalt oxide particles that could not be detected by XRD even for a cobalt loading as high as 8 wt%. These cobalt particles were small enough to fit into the pores of MCM-41. However, they were found to chemisorb CO in only relatively small amounts and to have low activities for CO hydrogenation—probably due to the formation of cobalt silicates. The use of cobalt chloride resulted in very large cobalt particles/clusters and/or residual Cl⁻-blocking active sites, and, consequently, very small active surface area was measurable. The use of cobalt nitrate resulted in a number of small cobalt particles dispersed throughout MCM-41 and some larger particles located on the external surface of MCM-41. Cobalt nitrate appeared to be the best precursor for preparing high-activity MCM-41-supported cobalt Fischer–Tropsch synthesis catalysts.

KEY WORDS: cobalt catalyst preparation; cobalt precursors; MCM-41; CO hydrogenation.

1. Introduction

Co-based catalysts are widely used in CO hydrogenation or Fischer–Tropsch synthesis (FTS), especially when high molecular weight paraffins are preferred [1–3]. To increase their activity, cobalt is usually deposited on a high surface area support to obtain a high metal dispersion. The commonly used supports include silica [4–6], alumina [7–9], and titania [10,11]. Recently, attention has been focused on the use of ordered mesoporous materials such as MCM-41 as catalyst supports. MCM-41 possesses excellent support properties such as high BET surface area and well-ordered hexagonal pore structures that can be tailor-made in the pore-diameter range of 1.5–10 nm [12,13]. Their thermal and hydrothermal stability have also been improved by changing the synthesis chemicals and/or reaction conditions [14,15]. Many studies have reported significant improvements when these mesoporous materials were used as supports for catalyst preparation compared to conventional and commercial catalysts. For example, Song and Reddy [16] reported that Co-Mo supported on aluminosilicate MCM-41 prepared by impregnation showed higher hydrogenation and hydrocracking activities than conventional Co-Mo supported on γ-Al_2O_3. Schuth *et al.* [17] reported that Fe_2O_3/MCM-41 exhibited a superior performance for the conversion of SO_2 to SO_3 compared to Fe_2O_3 supported on conventional silica.

In a previous study [18], we reported the high Fischer–Tropsch activity of Ru-promoted MCM-41-supported cobalt catalysts. However, using incipient wetness impregnation with cobalt nitrate as the precursor resulted in cobalt being nonuniformly distributed on the MCM-41 support.

Besides the conventional impregnation technique, direct synthesis in which the metal ion source is introduced as a reactant into the synthesis gel and ion exchange has been widely used [19,20]. These methods, however, are limited by only small amounts of metal being able to be loaded and low metal dispersions [6]. Suvanto and coworkers reported high metal-loaded, well-dispersed Co/MCM-41 prepared using a gas-phase method and a fluidized-bed reactor [21]. This method is, however, more complicated than the conventional incipient wetness impregnation technique and may not be suitable for the preparation of commercial catalysts.

It is known that cobalt dispersion depends on the type of cobalt precursors. van de Loosdrecht *et al.* [22] showed that alumina-supported cobalt catalysts prepared by incipient wetness impregnation using cobalt EDTA and cobalt citrate precursors resulted in smaller cobalt oxide particles compared to the one prepared from cobalt nitrate. The use of cobalt oxalate, cobalt acetate, or cobalt acetylacetonate as cobalt precursors for titania-supported cobalt catalysts has been found to give higher cobalt dispersions than the catalysts prepared from cobalt nitrate [23]. Rosenek and Polansky [24] reported that use of cobalt acetate yields higher dispersion than cobalt chloride on silica. Sun *et al.* [25]

*To whom correspondence should be addressed.
E-mail: Joongjai.P@eng.chula.ac.th

concluded that catalysts prepared by mixed impregnation of cobalt nitrate and cobalt acetate result in higher Fischer–Tropsch synthesis activity than catalysts prepared from either monoprecursor. And recently, Soled *et al.* [26] has presented a comprehensive model for how precursor-support interactions influence the morphology and reducibility of the fresh cobalt catalysts. A balance between dispersion-enhancing strong support–precursor interaction and metal loss by retarded reduction was suggested.

However, less is known about the influence of cobalt precursors on the dispersion of cobalt when restricted pore-structure supports such as MCM-41 are used. The purpose of this study was to investigate the impact of different organic and inorganic cobalt precursors on cobalt dispersion in a restricted pore-structure support—in this case mesoporous MCM-41.

2. Experimental

2.1. Catalyst preparation

Pure silica MCM-41 was prepared in the same manner as that of Kruk *et al.* [27] using the following gel composition: $(1.0\,SiO_2) : (0.317\,TMAOH) : (0.45\,CTMABr) : (66.7\,H_2O)$, where TMAOH denotes tetramethylammonium hydroxide and CTMABr denotes cetyltrimethyl ammonium bromide. The Co/MCM-41 catalysts were prepared by the incipient wetness impregnation of the supports with aqueous solution of different cobalt precursors such as cobalt nitrate (Aldrich), cobalt acetate (APS), cobalt acetylacetonate (Aldrich) and cobalt chloride (Fluka). Cobalt loading was approximately 8% by weight of catalyst. The samples were dried at 110 °C for 1 day and were then calcined in air at 500 °C for 2 h. These catalysts with different cobalt precursors are respectively designated as Co/M-NO, Co/M-Cl, Co/M-AA, and Co/M-Ac, where Co/M refers to cobalt supported on MCM-41 and the last two letters reflect the type of the cobalt precursor used: NO for cobalt nitrate, Cl for cobalt chloride, AA for cobalt acetylacetonate, and Ac for cobalt acetate.

2.2. Catalyst characterization

2.2.1. Atomic adsorption spectroscopy

The bulk composition of cobalt was determined using a Varian Spectra A800 atomic adsorption spectrometer.

2.2.2. N_2 physisorption

The BET surface area, pore volume, average pore diameter, and pore-size distribution of the catalysts were determined by N_2 physisorption using a Micromeritics ASAP 2000 automated system. Each sample was degassed in the Micromeritics ASAP 2000 at 150 °C for 4 h prior to N_2 physisorption.

2.2.3. X-ray diffraction (XRD)

The XRD spectra of the catalysts were measured using a SIEMENS D5000 X-ray diffractometer, using Cu Kα radiation with a nickel filter in the 2–8° or 10–80°2θ angular regions.

2.2.4. Scanning electron microscopy (SEM)

Catalyst granule morphology and elemental distribution were obtained using a JEOL JSM-35CF scanning electron microscope. The SEM was operated at 20 kV. After the SEM micrographs were taken, elemental mappings were performed to determine the elemental concentration distribution on the catalyst granules using Link Isis 300 software. The catalyst samples were cut using an ultramicrotome in order to perform SEM-EDX on different spots of cross-sectioned catalyst granules.

2.2.5. Transmission electron microscopy (TEM)

The cobalt oxide particle size and the distribution of cobalt on MCM-41 were observed using a JEOL-TEM 200CX transmission electron microscope operated at 100 kV.

2.2.6. CO-pulse experiment

Relative percentages of cobalt dispersion were determined by pulsing carbon monoxide over the reduced catalyst. Approximately 0.2 g of catalyst was placed in a quartz tube, incorporated in a temperature-controlled oven and connected to a thermal conductivity detector (TCD). Prior to chemisorption, the catalyst was reduced in a flow of hydrogen (50 cc/min) at 400 °C for 2 h. Afterward, the sample was purged with helium at 400 °C for 1 h and finally cooled down to room temperature. Carbon monoxide was pulsed at 25 °C over the reduced catalyst until the TCD signal was constant.

2.2.7. Reaction test

CO hydrogenation was carried out at 220 °C and 1 atm total pressure in a fixed-bed stainless steel reactor under differential conversion conditions. A flow rate of $H_2/CO/Ar = 20/2/8\,cm^3/min$ was used. Typically, 0.2 g of the catalyst samples was reduced *in situ* in flowing H_2 (50 cc/min) at 350 °C for 10 h prior to the reaction. The product samples were taken at 1-h intervals and analyzed by gas chromatography. Steady state was reached after 6 h time onstream in all cases.

3. Results and discussion

To determine a suitable temperature for calcination of all cobalt precursors, thermogravimetric analysis (TGA) experiments were performed with bulk cobalt nitrate, cobalt acetate, cobalt acetyl acetonate, and cobalt chloride (figure 1). All cobalt precursors appeared to be fully decomposed for calcination
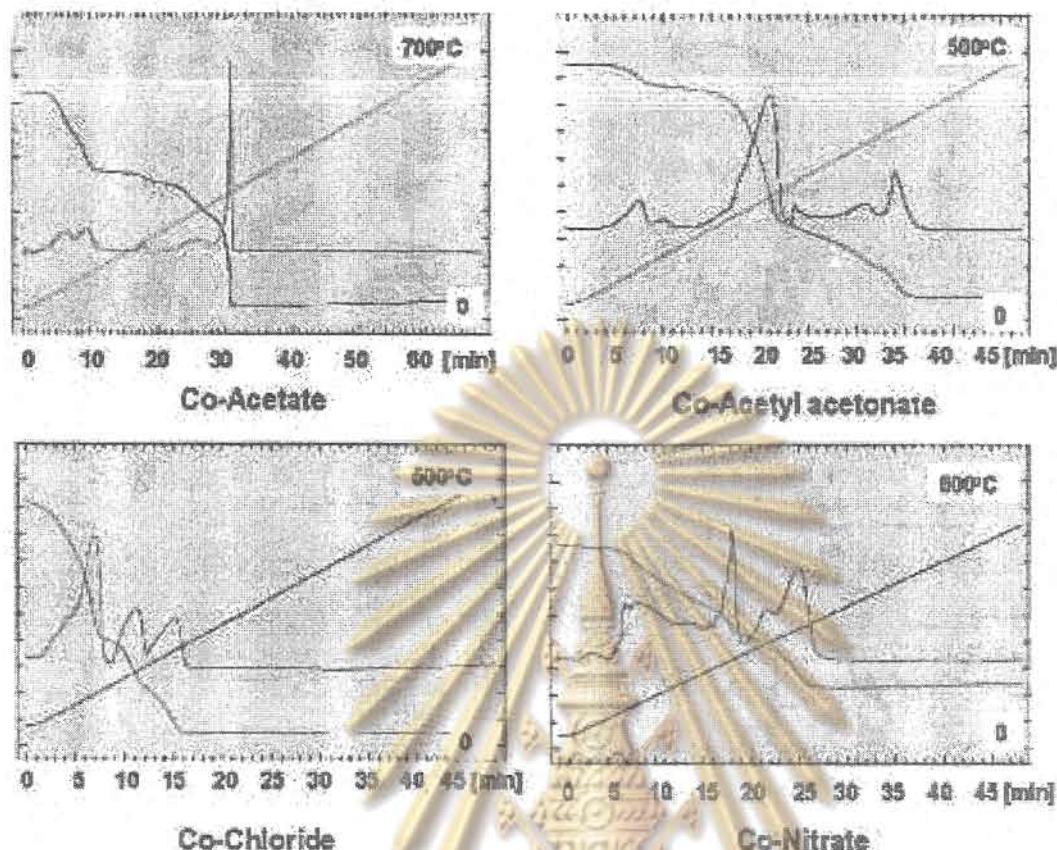
Figure 1. Thermogravimetric analysis (TGA) experiments for different cobalt precursors (bulk).

temperatures above 400 °C. Thus, a calcination procedure using 500 °C for 2 h was used to produce the cobalt oxide phase in all the various catalysts prepared.

The actual amounts of cobalt loading (determined by atomic adsorption spectroscopy), the BET surface areas, and the cobalt crystallite sizes (derived from XRD line broadening) for the catalyst samples are given in table 1. In this study, cobalt loading on the catalyst samples was approximately 7–8 wt% in order to make it close to that required for a commercial catalyst. The pure silica MCM-41 support before cobalt impregnation had a

Table 1
Characteristics of Co/MCM-41 catalysts prepared from different cobalt precursors

Catalyst	Co^a (wt%)	BET S.A.^{b} (m^2/g)	dp^c Co_3O_4 (nm)
MCM-41	—	1234	—
Co/M-Ac	8.3	756	<5
Co/M-AA	7.8	675	<5
Co/M-Cl	7.1	646	15.0
Co/M-NO	8.1	747	6.3

^{a}Elemental analysis using atomic adsorption spectroscopy. Error of measurement = ±2%.
^{b}Using N_2 physisorption at 77 K. Error of measurement = ±10%.
^{c}From XRD line broadening. Error of measurement = ±5%.

BET surface area of 1234 m^2/g and a pore volume of 0.85 cm^3/g. The BET surface areas of the cobalt catalysts prepared with different cobalt precursors were found to be in the range of 646–756 m^2/g and in the order of Co/M-Ac > Co/M-NO > Co/M-AA > Co/M-Cl. The significant decrease in surface area of the original support material suggests that cobalt was deposited significantly in the pores of MCM-41. The cobalt precursor did not have a significant impact on the average pore diameter of MCM-41 after cobalt loading since all the catalyst samples retained narrow pore-size distributions of approximately 3 nm, the same as the original MCM-41.

The XRD patterns of the MCM-41-supported cobalt catalysts are shown in figure 2. The ordered structure of MCM-41 gave an XRD peak at low 2θ around 2.58° for the unsupported MCM-41. After impregnation of cobalt, the intensity of the XRD peaks for MCM-41 was decreased for all the catalyst samples and the peaks became broader owing to the structure of MCM-41 becoming less ordered by the impregnation of cobalt or because of the secondary scattering of the X rays. The structure of MCM-41 was not destroyed, but the long-range order of MCM-41 may have shrunk [28].

The XRD patterns at higher diffraction angles of the MCM-41-supported cobalt catalysts prepared with
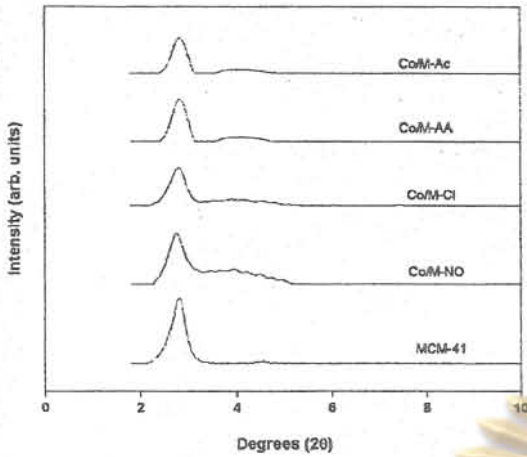
Figure 2. Effect of cobalt precursors on the XRD patterns of Co/MCM-41 catalysts (low 2θ).

different cobalt precursors in the calcined state are shown in figure 3. Co/M-NO and Co/M-Cl exhibited diffraction peaks at 2θ of ca. 31.3°, 36.8°, 45.1°, 59.4°, and 65.4°, indicating the presence of Co_3O_4 spinel in the catalyst particles. Surprisingly, Co/M-Ac and Co/M-AA did not exhibit any distinct XRD patterns. This suggests that the crystallite size of cobalt oxide prepared from cobalt acetate and cobalt acetylacetonate on MCM-41 was below the lower limit for XRD detectability (5 nm) even though cobalt loading was as high as 8 wt%. It is also possible that on Co/M-Ac and Co/M-AA, cobalt did not form Co_3O_4 crystallites but may have formed an amorphous cobalt oxide similar to what has been

suggested for Co/TiO_2 prepared from cobalt EDTA [23]. For Co/M-NO and Co/M-Cl, the average cobalt oxide crystallite sizes calculated using the Scherrer's equation [29] were found to be 6.3 and 15.0 nm, respectively. These cobalt particles were much larger than the average pore diameter of MCM-41 (3 nm), suggesting that using cobalt nitrate and cobalt chloride precursors to prepare MCM-41-supported cobalt catalysts by incipient wetness impregnation resulted in some large cobalt oxide particles deposited on the external surface of MCM-41.

SEM and elemental mapping were carried out for all the catalyst samples. Typical SEM micrographs of catalyst granules are shown in figure 4. The term "granule" here refers to a catalyst particle composed of cobalt and silica. In all the SEM figures, the white or light spots on the catalyst granules represent a high concentration of cobalt and its compounds, while the darker areas of the granules indicate the support with minimal/no cobalt present. The dark background is due to the carbon tape used for holding the catalyst samples. The SEM micrographs for catalyst granules prepared with different cobalt precursors show similar catalyst granule sizes of 30–50 μm. The elemental mappings for cobalt are shown in figure 5. The presence of very large cobalt clusters nonuniformly distributed on the granule exteriors was observed for Co/M-Cl. Dispersion of the cobalt was better for the other catalysts.

SEM-EDX was performed on cross-sectioned catalyst granules in order to determine the cobalt concentration at different locations on the catalyst granules (in the pores versus on the external surface). The SEM
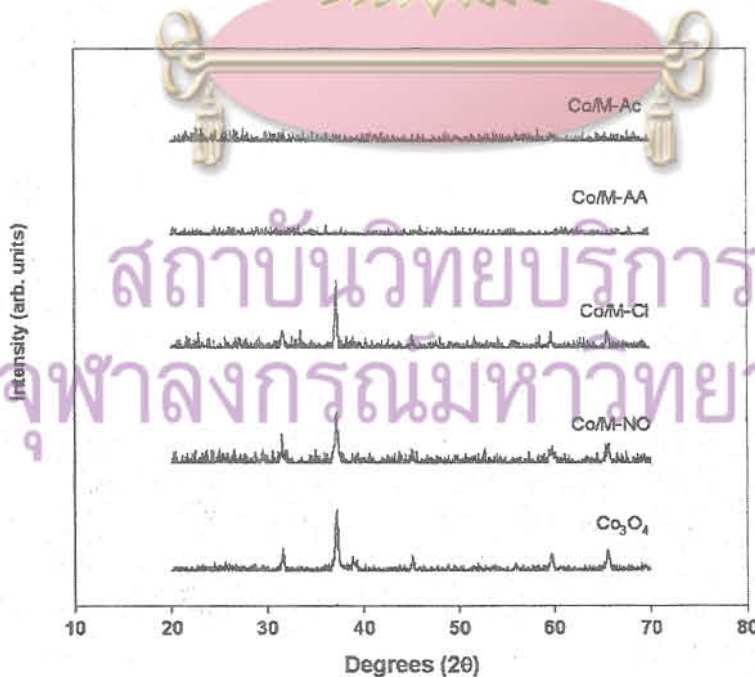

Figure 3. Effect of cobalt precursors on the XRD patterns of Co/MCM-41 catalysts (high 2θ).
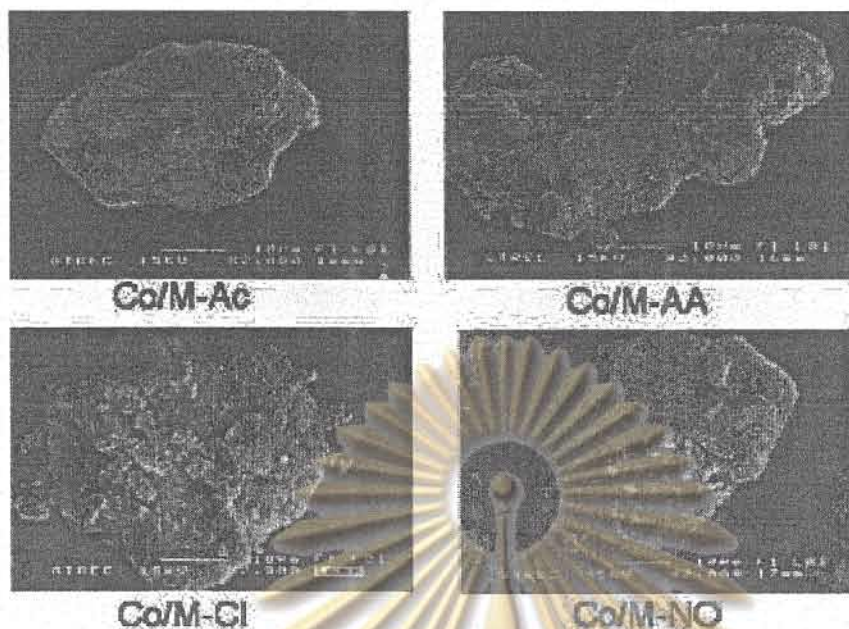
Figure 4. SEM micrographs of Co/MCM-41 catalysts prepared with different cobalt precursors.

micrographs of cross-sectioned catalyst granules with locations of EDX analysis are shown in figure 6. The corresponding elemental distributions are reported in table 2. Again, we observed a very high concentration of cobalt on the external surface of Co/M-Cl, whereas distribution of cobalt for the other catalysts was not significantly different across the cross-sectioned granules. SEM-EDX results thus confirm that, except for

Figure 5. Distribution of cobalt on the exteriors of different Co/MCM-41 catalyst granules from SEM elemental mappings.
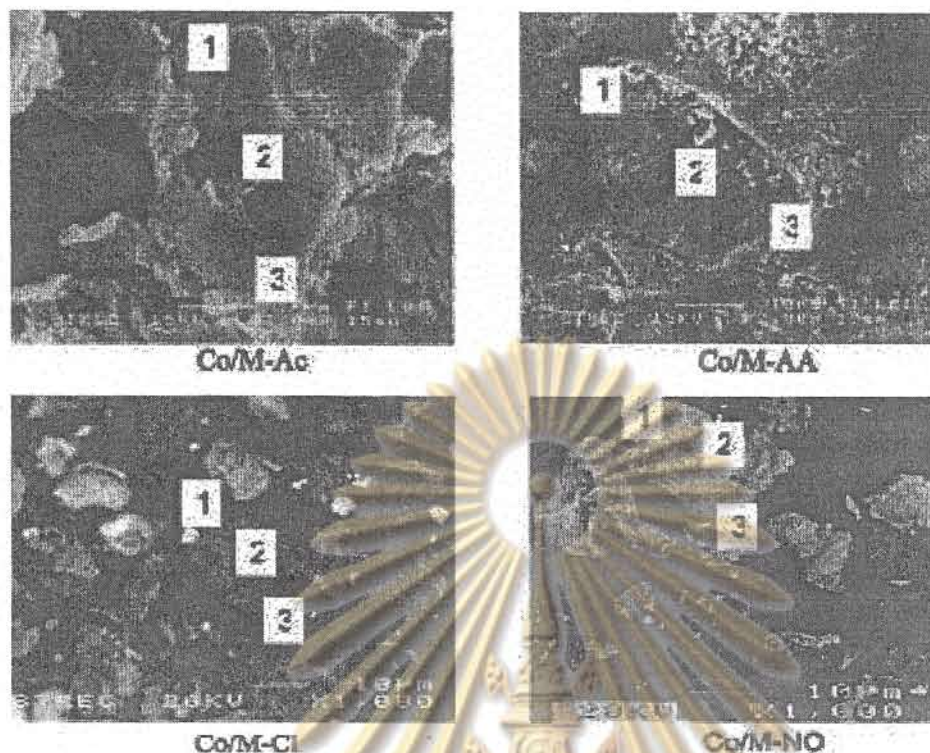
Figure 6. SEM micrograph of the cross-sectioned catalysts with locations of EDX analysis.

Co/M-Cl, the cobalt catalysts had their cobalt primarily located in the pores of MCM-41.

TEM micrographs were taken for all the catalysts in order to physically measure the size of cobalt oxide particles and/or cobalt clusters (figure 7). TEM images were found to be in accordance with the results from XRD and EDX that very large cobalt clusters $(1-2 \mu m)$ were present on Co/M-Cl, while dispersion of the cobalt was better for the other catalysts. Although TEM measurements were only done for a very small portion of each catalyst, the results are able to provide further evidence about cobalt dispersion.

The degrees of reduction, the relative rankings of cobalt dispersion, and the CO hydrogenation rates of the catalysts are reported in table 3. The degrees

Table 2

Elemental analysis using SEM-EDX on different locations of the cross-sectioned catalysts

Catalyst	Co (wt%)[a]		
	Location 1	Location 2	Location 3
Co/M-Ac	7.5	10.6	7.8
Co/M-AA	11.4	12.4	6.5
Co/M-Cl	18.6	4.9	6.9
Co/M-NO	7.9	6.0	7.7

[a]Error of measurement = ±10%.

of reduction of the catalysts in the TGA experiments from 30–800 °C were not significantly different, ranging from 53–64%, with Co/M-NO showing the highest degree of reduction. Any cobalt not reducible during the H_2 reduction up to 800 °C is identified as "nonreducible" cobalt silicate [30,31].

The relative ranking of cobalt dispersion was calculated from CO-pulse chemisorption experiments. Since for CO chemisorption on cobalt, bridge bonding may occur, there is no precise ratio of CO molecules to cobalt metal surface atoms that can be used. However, for strictly identical measurement conditions, CO chemisorption can yield a relative ranking of cobalt dispersion. It was found that CO chemisorption was only measurable for Co/M-AA and Co/M-NO, with Co/M-AA exhibiting higher amount of CO chemisorption than Co/M-NO. Co/M-Cl exhibited negligible chemisorption probably due to its low dispersion of cobalt and/or due to residual Cl$^-$ blocking the cobalt sites. Residual Cl$^-$ has been found in other supported metal catalysts when Cl-containing compounds are used as the catalyst precursor [32–34]. Figure 8 shows the XRD pattern of bulk $CoCl_2$ after calcination at 500 °C, where residual Cl$^-$ can be observed. However, residual Cl$^-$ was probably highly dispersed or present in very low amounts so that it could not be detected by XRD in case of the Co/M-Cl catalyst. One should note that residual Cl$^-$ has been shown to be significantly decreased in metal catalysts when water vapor is
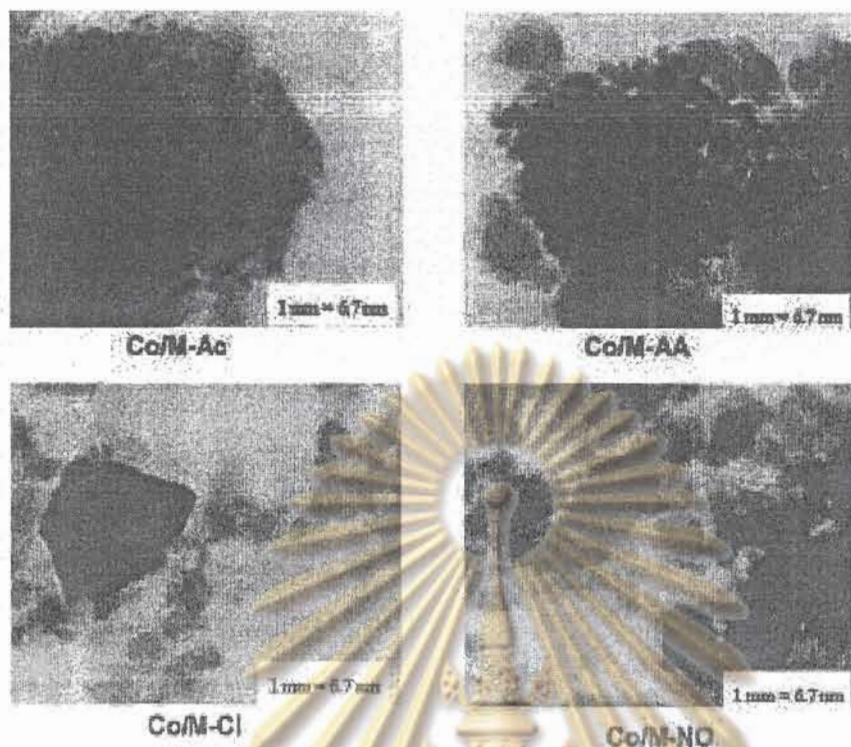
Figure 7. TEM micrographs of Co/MCM-41 catalysts prepared with different cobalt precursors.

present, such as during CO hydrogenation. Co/M-Ac had well-dispersed cobalt as determined by XRD and TEM; therefore, it is surprising that no CO adsorption could be measured at the conditions used.

The test reactions for CO hydrogenation were carried out at 220 °C, 1 atm, and H_2/CO ratio = 10 for all catalyst samples. A relatively high H_2/CO ratio was used in order to minimize deactivation due to carbon deposition during reaction. It was found that at the reaction conditions used, Co/M-NO exhibited a much higher CO hydrogenation rate than all other catalysts in this study. The low activity of Co/M-Ac and Co/M-AA is probably due to the unstable small cobalt particles forming cobalt silicates during reduction in H_2 [31,35] due to the water vapor generated.

The results of this study were found to be in agreement with the well-established trends in the literature on the influence of cobalt precursors on different supported cobalt Fischer–Tropsch catalysts [22–26]. It should be emphasized that our results support the need for a balance between dispersion-enhancing, strong support-precursor interaction and loss of metallic cobalt as a result of metal-support compound formation in order to obtain high-activity-supported cobalt catalysts, in agreement with the recent suggestions of Soled et al. [26]. The type of cobalt precursor must be carefully chosen, especially when restricted pore-structure supports such as MCM-41 are used. Cobalt particles small enough to fit into the pores of MCM-41 could be unstable at commercially relevant

Table 3
Results from TGA, CO-pulse chemisorption, and CO hydrogenation reaction

Catalyst	Reducibility[a] (30–800 °C)	CO chemisorption $(CO/Co)^b \times 100$	Rate[c] $\times 10^4$ ($g_{CH_2}/g_{cat}/h$)	
			Initial	Steady state
Co/M-Ac	59	Nil	0.068	0.057
Co/M-AA	53	7.6	0.338	0.071
Co/M-Cl	58	Nil	0.012	0.050
Co/M-NO	64	2.6	1.810	1.150

[a]From thermogravimetric experiments.
[b]The relative %Co dispersion from pulse CO chemisorption experiments.
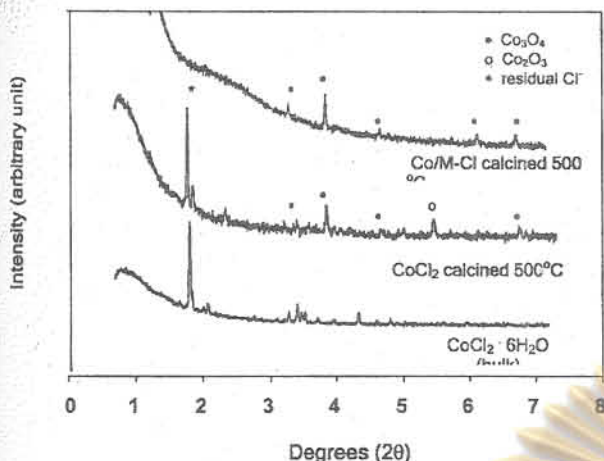[c]CO hydrogenation was carried out at 220 °C, 1 atm, $H_2/CO = 10$ ($H_2/CO/Ar = 20/2/8$ cc/min).

Figure 8. XRD pattern of residual Cl⁻ after calcination at 500 °C for 2 h.

synthesis conditions and thus have limited practical use.

4. Conclusion

Using organic precursors such as cobalt acetate or cobalt acetylacetonate instead of inorganic ones such as cobalt nitrate or cobalt chloride results in very small cobalt particles uniformly distributed throughout the pore structure of MCM-41. Extremely large cobalt particles/clusters are evident on Co/MCM-41 prepared from cobalt chloride. The results suggest, however, that there may be an optimum cobalt particle size and dispersion to maximize the surface cobalt availability since cobalt silicate formation during reduction may occur (especially for highly dispersed cobalt) and result in lower CO hydrogenation activity. Only surface cobalt metal atoms are active for CO hydrogenation. Among the four types of cobalt compounds used in this study, cobalt nitrate seems to be the best (optimum) cobalt precursor to prepare MCM-41-supported cobalt catalysts with significant CO hydrogenation activity at commercially relevant synthesis conditions.

Acknowledgment

References

[1] R.B. Anderson, *The Fischer–Tropsch Synthesis* (Academic Press, San Diego, 1984).
[2] J.G. Goodwin Jr., Prep. ACS Div. Petr. Chem. 36 (1991) 156.
[3] E. Iglesia, Appl. Catal. A 161 (1997) 50.
[4] R.C. Reuel and C.H. Bartholomew, J. Catal. 85 (1984) 78.
[5] L.B. Backman, A. Rautiainen, A.O.I. Krause and M. Lindblad, Catal. Today 43 (1998) 11.
[6] G.J. Haddad and J.G. Goodwin Jr., J. Catal. 157 (1995) 25.
[7] J. van de Loosdrecht, M. van der Haar, A.M. van der Krann and J.W. Geus, Appl. Catal. A 150 (1997) 365.
[8] A.R. Belambe, R. Oukaci and J.G. Goodwin Jr., J. Catal. 166 (1997) 8.
[9] D. Schanke, A.M. Hilmen, E. Bergene, K. Kinnari, E. Rytten, E. Adnanes and A. Holmen, Catal. Lett. 34 (1995) 269.
[10] J.H.A. Martens, H.F.J. van't Blik and R. Prins, J. Catal. 97 (1986) 200.
[11] J. Li and N.J. Coville, Appl. Catal. A 181 (1999) 201.
[12] J.S. Beck, J.C. Vartuli, W.J. Roth, M.E. Leonowicz, C.T. Kresge, K.D. Schmitt, C.T.-W. Chu, D.H. Olson, E.W. Sheppard, S.B. McCullen, J.B. Higgins and J.L. Schlenker, J. Am. Chem. Soc. 114 (1992) 10834.
[13] C.T. Kresge, M.E. Leonowicz, W.J. Roth, J.C. Vartuli and J.S. Beck, Nature 359 (1992) 710.
[14] E. Zhao, J. Feng, Q. Huo, N. Melosh, G.H. Fredrickson, B.F. Chmelka and G.D. Stucky, Science 279 (1998) 548.
[15] E. Zhao, Q. Huo, J. Feng, B.F. Chmelka and G.D. Stucky, J. Am. Chem. Soc. 120 (1998) 6024.
[16] C. Song and K.M. Reddy, Appl. Catal. A 176 (1999) 1.
[17] F. Schuth, A. Wingen and J. Sauer, Microporous and Mesoporous Mater. 44–45 (2001) 465.
[18] J. Panpranot, J.G. Goodwin Jr. and A. Sayari, J. Catal. 211 (2002) 530.
[19] A. Jentys, N.H. Pham, H. Vinek, M. Englisch and J.A. Lercher, Microporous Mater. 6 (1996) 13.
[20] A. Jentys, N.H. Pham, H. Vinek, M. Englisch and J.A. Lercher, Catal. Today 39 (1998) 311.
[21] S. Suvanto, J. Hukkamaki, T.T. Pakkanen and T.A. Pakkanen, Langmuir 16 (2000) 4109.
[22] J. van der Loosdrecht, M. van der Haar, A.M. van der Kraan, A.J. van Dillen and J.W. Geus, Appl. Catal. A 150 (1997) 365.
[23] M. Kraum and M. Baerns, Appl. Catal. 186 (1999) 189.
[24] M.P. Rosynek and C.A. Polansky, Appl. Catal. 73 (1991) 97.
[25] S. Sun, N. Tsubaki and K. Fujimoto, Appl. Catal. A 202 (2000) 121.
[26] S.L. Soled, E. Iglesia, R.A. Fiato, J.E. Baumgartner, H.B. Vroman and S. Miseo, Paper 293, *18th North American Catalysis Society Meeting*, Cancun, Mexico, 1–6 June 2003.
[27] M. Kruk, M. Jaronice and A. Sayari, Microporous Mesoporous Mater. 35–36 (2000) 545.
[28] L. Pasqua, F. Testa, R. Aiello, F. Di Renzo and F. Fajula, Microporous and Mesoporous Mater. 44–45 (2001) 111.
[29] H.P. Klug and L.E. Alexander, *X-ray Diffraction Procedures for Polycrystalline Amorphous Materials*, 2nd ed. (Wiley, New York, 1974).
[30] L.B. Backman, A. Rautiainen, A.O.I. Krause and M. Lindblad, Catal. Today 43 (1998) 11.
[31] A. Kogelbauer, J.C. Webber and J.G. Goodwin Jr., Catal. Lett. 34 (1995) 259.
[32] N. Mahata and V. Vishwanathan, J. Catal. 196 (2000) 262.
[33] Y. Zhou, M.C. Wood and N. Winograd, J. Catal. 146 (1994) 82.
[34] P. Johnston and R.W. Joyner, J. Chem. Soc. Faraday Trans. 89 (1993) 863.
[35] J.M. Jablonski, M. Wolcyrz and L. Krajczyk, J. Catal. 173 (1998) 530.

Co-support compound formation in titania-supported cobalt catalyst

Bunjerd Jongsomjit[a,*], Chitlada Sakdamnuson[a], James G. Goodwin Jr[b], and Piyasan Praserthdam[a]

[a]*Center of Excellence on Catalysis and Catalytic Reaction Engineering, Department of Chemical Engineering, Faculty of Engineering, Chulalongkorn University, Bangkok 10330, Thailand*
[b]*Department of Chemical Engineering, Clemson University, Clemson, SC 29634, USA*

Co-support compound formation (Co-SCF) in Co/TiO_2 was found during standard reduction resulting in a lower reducibility of the catalyst. The compound formed is considered to be non-reducible at temperatures <800 °C during TPR and different from $CoTiO_3$. The characteristics of Co-SCF were investigated using BET surface area, XRD, Raman spectroscopy, SEM/EDX, and TPR.

KEY WORDS: supported catalyst; cobalt catalyst; cobalt-support compound; titania support; Co/TiO_2; reducibility; CO hydrogenation.

1. Introduction

In Fischer–Tropsch synthesis (FTS), supported cobalt catalysts are preferred because of their high activity for FTS based on natural gas [1], high selectivity to linear long-chain hydrocarbons and low activity for the water–gas shift (WGS) reaction [2,3]. However, compound formation between cobalt and the supports can occur during the catalyst activation and/or reaction conditions resulting in irreversible catalyst deactivation [4–6].

Besides alumina (Al_2O_3) and silica (SiO_2), titania (TiO_2) has been widely studied as the support for cobalt catalysts by many authors [7–20], especially for the application of FTS in a continuously stirred tank reactor (CSTR) [11,15]. It was reported that Co-SCF in SiO_2 [21] and Al_2O_3 [4–6,22] can occur during standard reduction and resulted in a lower degree of reduction. However, titania was the first support where strong metal support interaction was observed [19]. In the present research, the nature of Co-SCF in titania-supported cobalt catalyst and its effect on the characteristics of the catalysts were the main focus. In this study, the Co/TiO_2 catalyst was prepared, pretreated under various conditions, and characterized using BET surface area, XRD, TPR, SEM/EDX, and Raman spectroscopy to identify the nature of compounds formed. The main objectives of this research were to develop a better understanding of Co-SCF in titania-supported cobalt catalyst and to better identify the compounds formed. Based on information obtained from the present research, the strategies to minimize such a compound formation can be further developed.

*To whom correspondence should be addressed.
E-mail: bunjerd.j@chula.ac.th

2. Experimental

2.1. Catalyst preparation

A 20 wt% of Co/TiO_2 was prepared by the incipient wetness impregnation. A designed amount of cobalt nitrate [$Co(NO_3) \cdot 6H_2O$] was dissolved in deionized water and then impregnated onto TiO_2 (anatase form calcined at 600 °C obtained from Ishihara Sangyo, Japan). The catalyst precursor was dried at 110 °C for 12 h and calcined in air at 500 °C for 4 h.

2.2. Catalyst pretreatments

Standard reduction of the calcined catalyst was conducted in a fixed-bed flow reactor under differential conditions at 1 atm using a temperature ramp from ambient to 350 °C at 1 °C/min and holding at 350 °C for 10 h in a gas flow having a space velocity of 16,000 h^{-1} and consisting of H_2 or mixtures of H_2 and water vapor (5–10 vol%). The high space velocity of the H_2 flow when water vapor was not added insured that the partial pressure of water vapor in the catalyst bed produced by cobalt oxide reduction would be essentially zero in that case. The reduced catalyst was then passivated at room temperature with air for 30 min.

2.3. Catalyst nomenclature

The nomenclature used for the catalyst samples in this study is following:

- Co–C: the calcined catalyst sample
- Co–RW0: the calcined catalyst sample reduced in H_2
- Co–RW5: the calcined catalyst sample reduced in a mixture of H_2 with 5 vol% water vapor added during reduction
- Co–RW10: the calcined catalyst sample reduced in a mixture of H_2 with 10 vol% water vapor added during reduction

2.4. Catalyst characterization

2.4.1. BET surface area
BET surface area of the samples after various pretreatments was performed to determine if the total surface area changes upon the various pretreatment conditions. It was determined using N_2 adsorption at 77 K in a Micromeritics ASAP 2010.

2.4.2. X-ray diffraction
XRD was performed to determine the bulk crystalline phases of catalyst following different pretreatment conditions. It was conducted using a SIEMENS D–5000 X-ray diffractometer with CuK_α ($\lambda = 1.54439$ Å). The spectra were scanned at a rate of 2.4 °/min in the range $2\theta = 20$–$80°$.

2.4.3. Scanning electron microscopy and energy dispersive X-ray spectroscopy
SEM and EDX were used to determine the catalyst morphologies and elemental distribution throughout the catalyst granules, respectively. The SEM of JEOL mode JSM–5800LV was applied. EDX was performed using Link Isis series 300 program.

2.4.4. Raman spectroscopy
The Raman spectra of the samples were collected by projecting a continuous wave laser of argon ion (Ar^+) green (514.532 nm) through the samples exposed to air at room temperature. A scanning range of 100–1000 cm^{-1} with a resolution of 2 cm^{-1} was applied. The data were analyzed using the Renishaw WiRE (Windows-based Raman Environment) software, which allows Raman spectra to be captured, calibrated, and analyzed using system 2000 functionality via Galactic GRAMS interface with global imaging capacity.

2.4.5. Temperature-programmed reduction
TPR was used to determine the reduction behaviors and reducibilities of the samples. It was carried out using 50 mg of a sample and a temperature ramp from 35 to 800 °C at 5 °C/min. The carrier gas was 5% H_2 in Ar. A cold trap was placed before the detector to remove water produced during the reaction. A thermal conductivity detector (TCD) was used to determine the amount of H_2 consumed during TPR. The H_2 consumption was calibrated using TPR of Ag_2O at the same conditions. The reduced samples were recalcined at the original calcination conditions prior to performing TPR. The calculation of reducibilities was described elsewhere [4–6,21,22,23].

2.5. Reaction

CO hydrogenation ($H_2/CO = 10/1$) was performed to determine the overall activity of the catalyst samples reduced at various conditions. Hydrogenation of CO was carried out at 220 °C and 1 atm. A flow rate of H_2/

CO/He = 20/2/8 cc/min in a fixed-bed flow reactor under differential conditions was used. A relatively high H_2/CO ratio was used to minimize deactivation due to carbon deposition during reaction. Typically, 20 mg of a catalyst sample was re-reduced in situ in flowing H_2 (30 cc/min) at 350 °C for 10 h prior to the reaction. Reactor effluent samples were taken at 1 h intervals and analyzed by GC. In all cases, steadystate was reached within 5 h.

3. Results and discussion

3.1. Evidence of Co-SCF in Co/TiO₂ catalyst

It can be observed that Co-SCF in Co/TiO_2 essentially occurred during standard reduction resulting in lower reducibilities of the reduced samples during TPR at temperatures 35–800 °C as shown in table 1. The reducibilities ranged from 92% to 64% upon the various pretreatments of catalyst samples. Essentially, TPR of the TiO_2 support only (table 1) was also conducted at the same condition and no hydrogen consumption was detected. It should be noted that the loss in the degree of reduction was attributed to the compound formation of cobalt and the titania support. The suggested conceptual diagram of reducibility loss during standard reduction is illustrated in figure 1. First, when performing TPR on a fresh calcined sample, the reducibility gain was 92%. However, when the calcined sample was reduced with and without water vapor addition (5–10 vol%) during reduction, then recalcined it back to the oxide form prior to performing TPR, the reducibilities obviously decreased. The reducibilities loss during the reduction process were found to be in the range of 22–28% indicating the non-reducible (at temperatures < 800 °C) "Co-titanate" compound formed. The term "Co-titanate" is used here to refer to the surface compound formed during standard reduction of cobalt and the titania support.
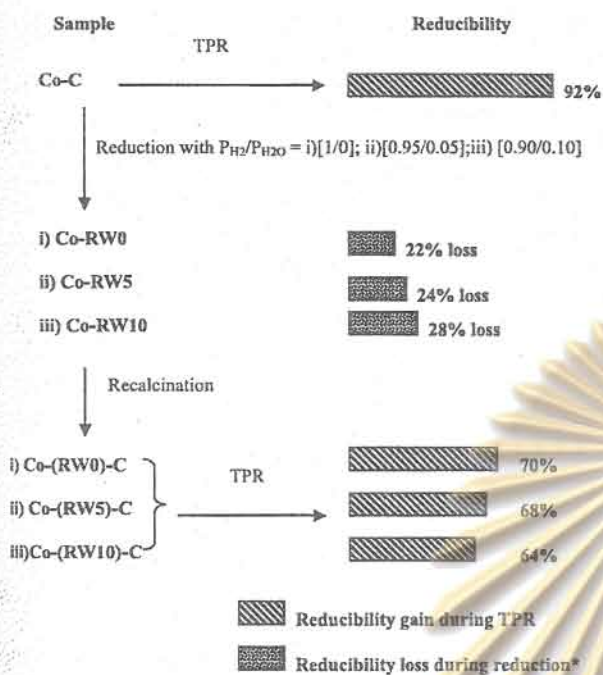
It should be mentioned that a decrease in the degree of reduction of reduced samples slightly changed upon

Table 1
Reducibilities and surface areas of samples after various pretreatments

Sample	Reduction gas mixture (P_{H2}/P_{H2O})	Reducibility (%) during TPR at 35–800 °C[a,b]	Surface area (m^2/g)[b]
TiO_2	–	–	70
Co–C	–	92	52
Co–RW0	1/0	70	49
Co–RW5	0.95/0.05	68	46
Co–RW10	0.90/0.10	64	46

[a]The reduced samples were recalcined at the original calcination conditions prior to performing TPR.
[b]Measurement error is ±5%.

Figure 1. Suggested conceptual diagram for the reducibility loss during reduction process.

* The difference in reducibility gain from a fresh calcined sample and the reducibility gain from a reduced and recalcined sample.

Figure 2. TPR profiles of bulk Co_3O_4 and the catalyst samples after various pretreatment conditions.

increasing the partial pressures of water vapor during the reduction process. Zhang et al. [22] investigated the reducibilities of $CoRu/\gamma-Al_2O_3$ during standard reduction and TPR in the presence of added water vapor. They reported that water has a significant effect on the reduction behavior of $CoRu/\gamma-Al_2O_3$. It was suggested that water vapor present during reduction leads to a decrease in the degree of reduction of the cobalt perhaps in two ways: (i) inhibition of the reduction of well-dispersed CoO interacting with the alumina support, possibly by increasing the cobalt–alumina interaction, and (ii) facilitation of the migration of cobalt ions into probable tetrahedral sites of $\gamma-Al_2O_3$ to form a non-reducible (at temperatures < 900 °C) spinel. However, considering the Co-SCF in Co/TiO_2, the effect of water vapor added during standard reduction was essentially less pronounced compared to that on the alumina support. The only slight effect of water vapor on Co-SCF in Co/TiO_2 is also listed in table 1 indicating that the reducibilities of the reduced samples only slightly decreased within experimental error when water vapor (5–10 vol%) was added during standard reduction. Besides the reducibility measurement, TPR also provides information on the reduction behaviors of the catalyst samples pretreated under various conditions.

TPR profiles of bulk Co_3O_4 and the catalyst samples after various pretreatment conditions are shown in figure 2. Only one strong reduction peak can be
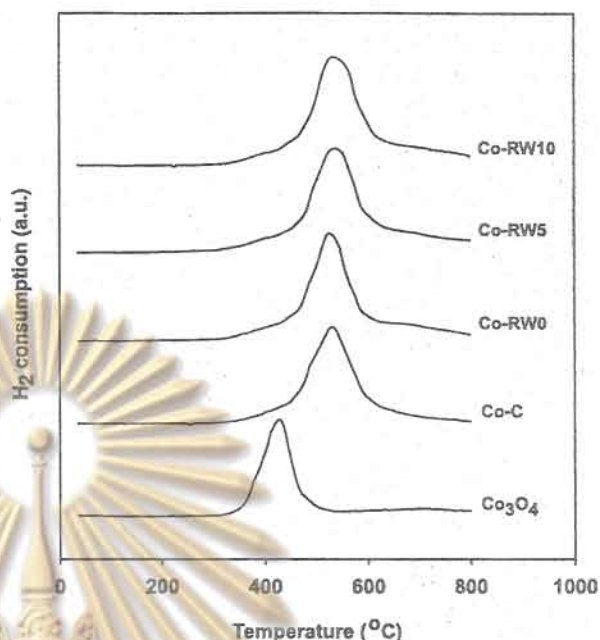
observed for bulk Co_3O_4 and all the samples regardless of various pretreatment conditions used. This peak can be assigned to the overlap of two-step reduction of Co_3O_4 to CoO and then to Co^0 [22,24,25]. Upon the TPR conditions, the two reduction peaks based on the two-step reduction may or may not be observed. The TPR profile of the titania support (not shown) showed no reduction peak. There was only one reduction peak located at ca. 370–620 °C (max. at 520 °C) for the calcined sample (Co–C) indicated that no residual cobalt nitrates remain on the calcined sample of Co/TiO_2 upon the calcination condition used in this study. In some cases, the peak of the decomposition of cobalt nitrates during TPR of supported cobalt catalysts can be observed at temperatures between 200 and 300 °C, especially with silica and alumina supports [4–6,23,26,27]. However, prolonged calcination or reduction and recalcination results in complete decomposition of any cobalt nitrates present [23].

TPR profiles of all reduced samples were also similar exhibiting only one reduction peak as shown in figure 2. TPR peak located at ca. 400–620 °C (max. at 520 °C) for Co-RW0 sample was slightly shifted about 10 °C higher when the partial pressure of water vapor was increased during reduction indicating slightly stronger interaction between cobalt and titania support. However, the much stronger interaction between cobalt and the supports such as silica and alumina can be usually observed leading to an observation of two separated peaks during TPR of the reduced and recalcined samples [4–6,21,23]. The higher temperature reduction peak can be assigned to the reduction of cobalt strongly interacting with the

supports, i.e. Co_xO_y–Al_2O_3 and Co_xO_y–SiO_2, which can not be observed in the reduced and recalcined Co/TiO_2 catalyst. Based on the TPR results, it should be noted that a degree of reduction of the reduced Co/TiO_2 catalyst was found to decrease during standard reduction due to "Co-titanate" formed. However, the reduction behaviors of samples reduced in various conditions were similar upon the TPR measurement conditions used in this study. This can be concluded that "Co-titanate" formed in a Co/TiO_2 catalyst resulted in only a decrease in the reducibility without changing the reduction behaviors of it. The effect of partial pressures of water vapor during reduction on the formation of "Co-titanate" seemed to be less pronounced.

3.2. Characteristics of "Co-titanate"

In order to identify the characteristics of "Co-titanate" formed during reduction, several characterization techniques were conducted. BET surface areas of TiO_2 and the catalyst samples after various pretreatments are also shown in table 1. BET surface areas of samples were slightly less than the titania (anatase form) support (70 m²/g). Since all surface areas of the samples in this study ranged between 46 and 52 m²/g, there was no significant change in surface areas after the various pretreatments within experimental errors. This indicated that "Co-titanate" formed did not cause any change in surface areas of the catalyst.

SEM and EDX were performed to study the morphologies of the catalyst samples and elemental distributions of the catalyst samples, respectively. There was no significant change in morphologies of catalyst samples due to the "Co-titanate" formed. By observation on the external surface of the catalyst granules, cobalt patches (the term "patches" is used to refer to the entities rich in cobalt supported on the catalyst granules) can be seen all over the external surface of samples. In general, all of them were similar regardless of the pretreatment conditions used. The typical morphology in an external area of catalyst granules with different magnification for Co-RW10 is shown in figure 3. It can be observed that cobalt patches (white spots) were well distributed all over the external surface of catalyst granules. The elemental distributions can be clearly seen by EDX. Figure 4 shows the typical elemental distribution for a cross section of a granule of Co-RW10. The distribution of cobalt was well dispersed throughout the catalyst granule as also seen by SEM. Thus, there was no significant change in catalyst morphologies and elemental distribution upon the formation of "Co-titanate".

The bulk crystalline phases of samples were determined using XRD. XRD patterns of TiO_2, $CoTiO_3$ (synthesized, based on reference [28]) and catalyst samples after various pretreatments are shown in figure 5. XRD patterns of TiO_2 showed strong diffrac-
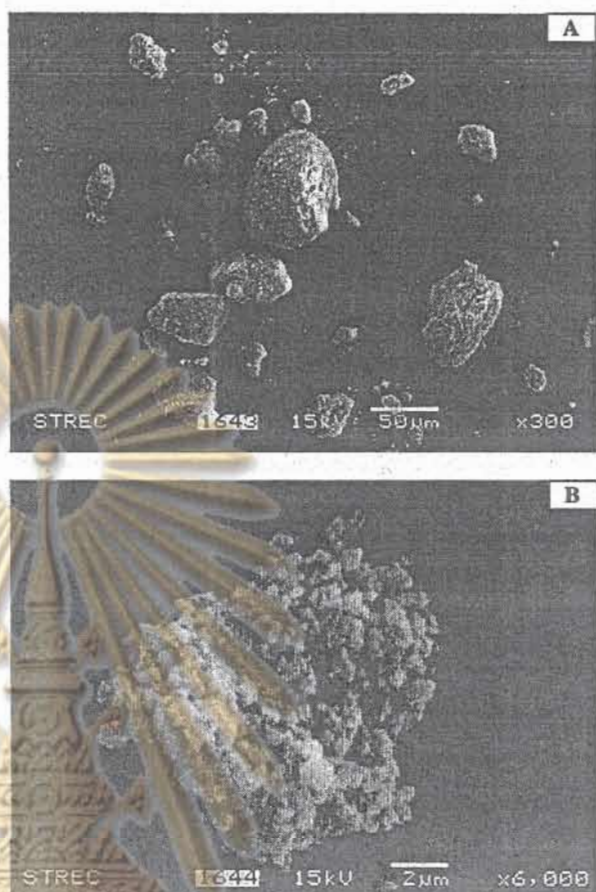
Figure 3. SEM micrographs of Co-RW10 catalyst granule at the external surface; (a) at 300× magnification and (b) at 6000× magnification.

tion peaks at 26°, 37°, 48°, 55°, 56°, 62°, 69°, 71° and 75° indicating the TiO_2 in the anatase form. After calcination, the diffraction peaks of Co_3O_4 at 36°, 46°, and 65° can be observed. Apparently, the relative intensity of those peaks is much lower compared to the TiO_2 peaks. To identify the XRD peaks of samples, XRD peaks of $CoTiO_3$ were also collected and it showed the diffraction peaks at 23°, 32°, 35°, 49°, 52°, 62° and 64° as also shown in figure 5. Kraum et al. [29] reported the observation for XRD peaks of $CoTiO_3$ phase along with Co_3O_4 on the calcined Co/TiO_2 catalyst using cobalt (III) acetyl acetonate as a precursor for cobalt. They suggested that the formation of $CoTiO_3$ by the use of cobalt (III) acetyl acetonate as a precursor can be attributed to the migration of cobalt ions into the support lattice, with the consecutive formation of titanate. However, based on differences in the cobalt precursor, the amounts of cobalt loading and the calcination condition used in the present study, the formation of $CoTiO_3$ was not observed in the calcined Co/TiO_2 catalyst. After reduction at various conditions and passivation, the diffraction peaks of CoO were
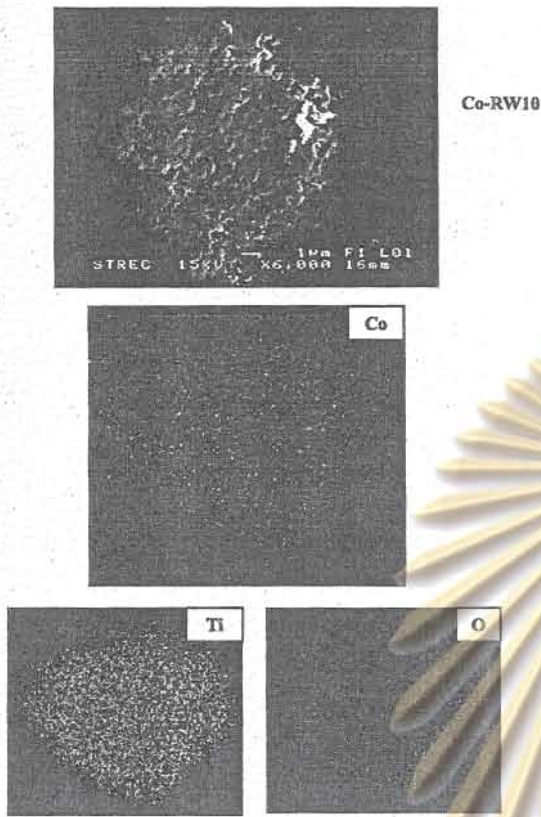
Figure 4. SEM micrograph and EDX mapping of Co-RW10 catalyst granule (cross section).

Figure 5. XRD patterns of TiO_2, $CoTiO_3$ and the catalyst samples after various pretreatment conditions.

present at 37° and 63°. This indicated that Co_3O_4 in the calcined samples was reduced to highly dispersed cobalt metal and CoO during standard reduction at 350 °C. Any Co_3O_4 formed during passivation was present in only very thin surface layers and was consequently XRD invisible. No XRD peaks for "Co-titanate" formed were detected for any of the catalyst samples. In order to investigate the structure of non-reducible (at temperatures < 800 °C during TPR) "Co-titanate", XRD was also conducted on the samples after performing TPR up to 800 °C. XRD patterns of samples after TPR measurement up to 800 °C are shown in figure 6. The similar trend as shown in figure 5 was found except for the observation of cobalt metal peaks at 44° and 52° due to sintering. No phase change, i.e from anatase to rutile form of TiO_2 was observed. XRD results revealed that the "Co-titanate" formed was in a highly dispersed form, thus it is invisible in XRD after either standard reduction or TPR.

Raman spectra of TiO_2, CoO, Co_3O_4, $CoTiO_3$ and the catalyst samples after various pretreatments are shown in figure 7. To identify Raman bands of samples, the Raman spectra of Co_3O_4, CoO and $CoTiO_3$ were collected. The Raman bands of $CoTiO_3$ exhibited bands at 695, 604, 455, 382, 336 and 266 cm^{-1} which are similar to the ones reported by Brik et al. [30]. The strong Raman
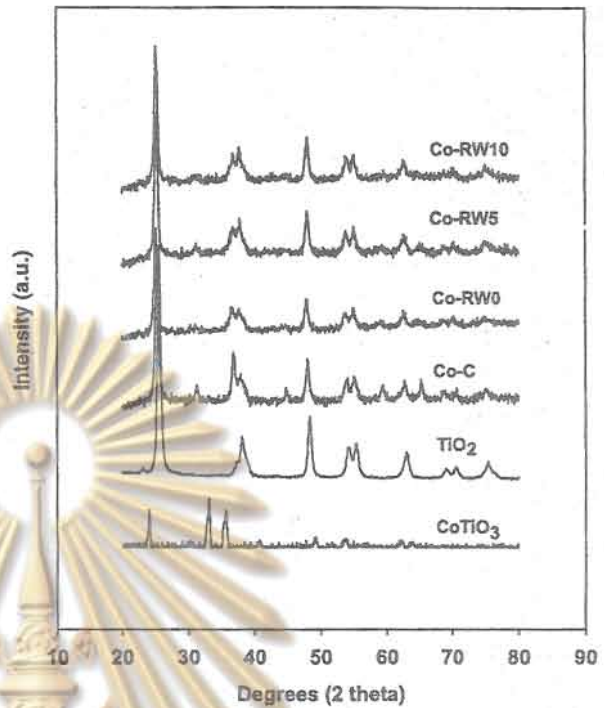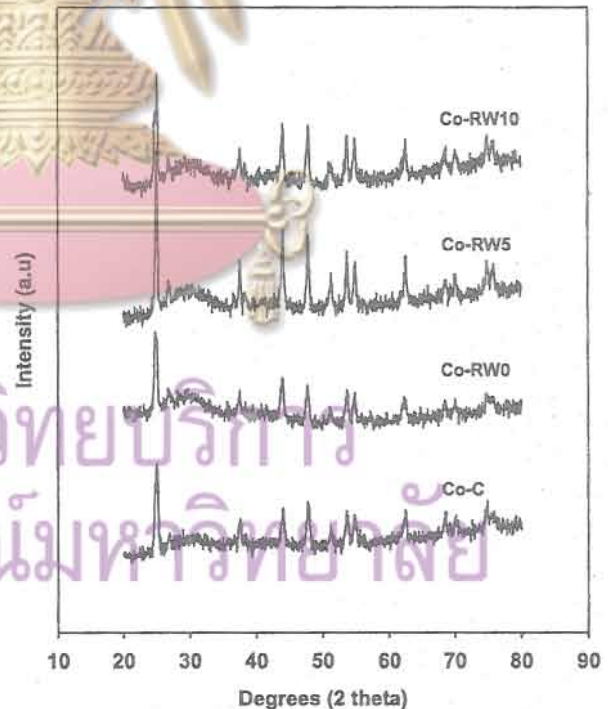

Figure 6. XRD patterns of the catalyst samples after TPR measurement up to 800 °C.

bands for TiO_2 were observed at 640, 514, and 397 cm^{-1} indicating the TiO_2 in its anatase form [9]. The Raman spectrum of the calcined sample exhibited Raman bands
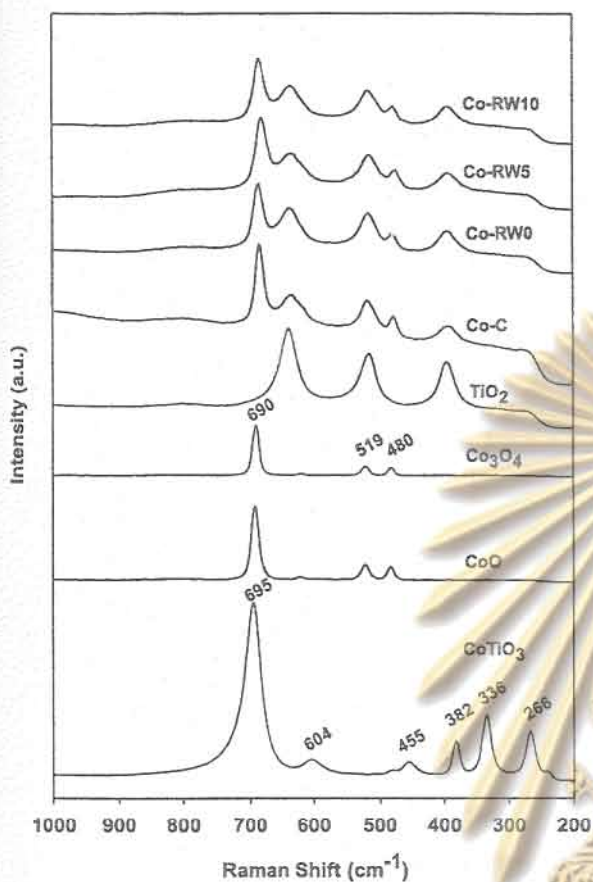
Figure 7. Raman spectra of TiO₂, Co₃O₄, CoO, CoTiO₃ and the catalyst samples after various pretreatment conditions.

Figure 8. Raman spectra of Co₃O₄, CoO, CoTiO₃, the calcined sample and the reduced with a lesser degree of passivation samples.

at 640, 514, and 397 cm⁻¹ as seen in those for TiO₂ including two shoulders at 690 and 480 cm⁻¹, assigned to Co₃O₄ [4–6]. Raman spectra of all reduced samples showed the Raman bands of TiO₂ support and the shoulders at 690 and 480 cm⁻¹. These can be assigned to Co₃O₄ present on catalyst surface rather than CoO (detected in the bulk by XRD) since Raman spectroscopy is more of surface technique [5]. This indicated that "Co-titanate" formed during reduction was different from CoTiO₃ and invisible in Raman spectroscopy. The invisible "Co-titanate" bands was probably caused by (i) its highly dispersed form and (ii) the Raman signals were hindered due to the highly strong Raman intensities of TiO₂ support. It was reported that reduced samples of Co/γ–Al₂O₃ at high partial pressure of water vapor during reduction exhibited the broad Raman bands between 400–700 cm⁻¹ [4]. This was suggested that these broad Raman bands represent a surface cobalt compound related to cobalt strongly interacting with the alumina support as a "Co-aluminate". The identified "Co-alumiante" was suggested to be different from CoAl₂O₄ (spinel) due to being a non-stoichiometric surface "Co-aluminate" compound. Thi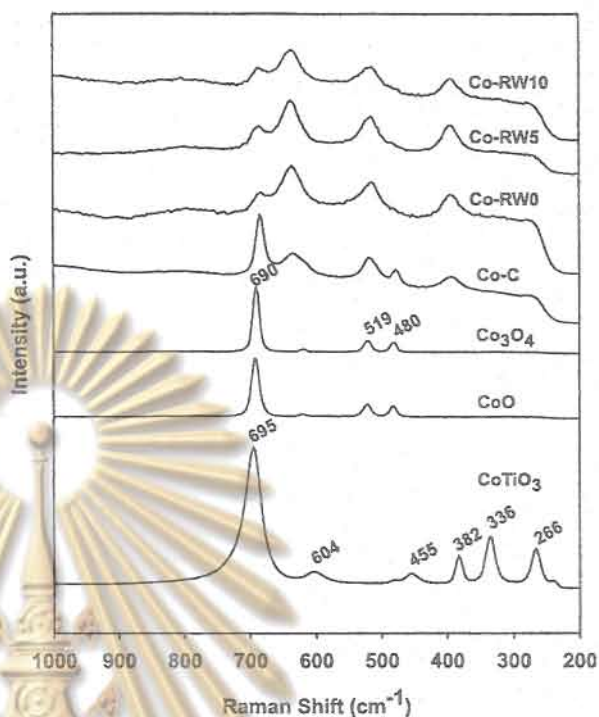s highly dispersed "Co-aluminate" may be formed, possibly by cobalt migration into the alumina matrix and was detectable using Raman spectroscopy, but not XRD. In addition, the alumina support itself does not exhibit any of Raman bands between 100 and 1000 cm⁻¹, thus, the Raman bands of "Co-aluminate" can be clearly detected. However, in the present study, the highly strong Raman intensities of the titania support may result in a hindrance of the Raman bands, if present, of the highly dispersed "Co-titanate" formed. Besides the strong signal of TiO₂, the signal of CoO and Co₃O₄ is likely to hinder the observation of surface "Co-titanate" as well. In order to eliminate that interference, we also conducted Raman spectroscopy on the reduced samples with a lesser degree of passivation and the Raman spectra of samples are shown in figure 8. It can be observed that the characteristic peaks of the reduced samples were similar to each other, but deviated from the characteristic peaks of Co₃O₄ as seen in figure 7. The Raman band of the reduced samples at 397 cm⁻¹ of the TiO₂ became broader. This perhaps resulted from the overlap between the peaks of 397 cm⁻¹ of the TiO₂ and 382 cm⁻¹ of CoTiO₃ due to the formation of surface "Co-titanate". However, to elucidate all kinds of hindrances, rigorous surface techniques may be needed for further investigation. Nevertheless, Raman spectroscopy revealed that the "Co-titanate" formed was different from CoTiO₃ probably due to it also being non-stoichiometric (cobalt deficiency) surface "Co-titanate" compound.

CO hydrogenation was performed to determine the overall activity of the catalyst samples reduced at

Table 2
Reaction rate for CO hydrogenation on catalyst samples reduced at various conditions

Sample	CO conversion (%)[a]		Rate (μmol/gcat.s)[b]		CH$_4$ selectivity (%)	
	Initial[c]	SS[d]	Initial	SS	Initial	SS
Co–C	3.71	2.09	1.39	0.79	99	99
Co–RW0	1.53	0.73	0.58	0.27	99	99
Co–RW5	0.83	0.46	0.31	0.17	99	99
Co–RW10	0.34	0.08	0.13	0.03	98	98

[a]CO hydrogenation was carried out at 220 °C, 1.8 atm, and H$_2$/CO/He = 20/2/8 cc/min).
[b]Error ±5%.
[c]After 5 min of reaction.
[d]After 5 h of reaction.

various conditions. The results are shown in table 2. It indicated that the CO conversion ranged between 3.71 and 0.34% (initial) and 2.09 to 0.08% (steady state). The reaction rate ranged between 1.39 and 0.13 μmol/g cat.s (initial) and 0.79–0.03 μmol/g cat.s (steady). This suggested that the "Co-titanate" formed in the reduced samples resulted in decreased activities of catalyst. However, there was no significant difference in selectivity for any of samples based on reaction conditions used in this study.

4. Conclusions

We have shown that Co-support compound formation (Co-SCF) in titania-supported cobalt catalyst can occur during standard reduction resulting in a lower reducibility of catalyst. The compound of cobalt and titania formed referred as "Co-titanate" was considered to be non-reducible at temperatures < 800 °C. The "Co-titanate" formed resulted in a decrease in the degree of reduction without any significant change in the reduction behaviors. It was found that the partial pressures of water vapor during reduction probably had only a slight effect on an increase in the "Co-titanate" formation. Due to its highly dispersed form, it can not be detected by XRD. However, Raman spectroscopy revealed that this highly dispersed "Co-titanate" formed was likely to be different from CoTiO$_3$ and present as a non-stoichiometric surface "Co-titanate" compound. The "Co-titanate" formed also resulted in decreased activities of catalyst without any changes in selectivity.

Acknowledgments

References

[1] H.P. Wither Jr., K.F. Eliezer and J.W. Michell, Ind. Eng. Chem. Res. 29 (1990) 1807.
[2] E. Iglesia, Appl. Catal. A 161 (1997) 59.
[3] R.C. Brady and R.J. Pettit, J. Am. Chem. Soc. 103 (1981) 1287.
[4] B. Jongsomjit, J. Panpranot and J.G. Goodwin Jr., J. Catal. 204 (2001) 98.
[5] B. Jongsomjit and J.G. Goodwin Jr., Catal. Today 77 (2002) 191.
[6] B. Jongsomjit, J. Panpranot and J.G. Goodwin Jr., J. Catal. 205 (2003) 66.
[7] W.S. Epling, P.K. Cheekaamarla and A.M. Lane, Chem. Eng. J. 93 (2003) 61.
[8] A. Voβ, D. Borgmann and G. Wedler, J. Catal. 212 (2002) 10.
[9] Y. Brik, M. Kacimi, F. Bozon-Verduraz and M. Ziyad, J. Catal. 211 (2002) 470.
[10] D.J. Duvenhage and N.J. Coville, Appl. Catal. A 233 (2002) 63.
[11] J.L. Li, G. Jacobs, T. Das and B.H. Davis, Appl. Catal. A 233 (2002) 255.
[12] K. Nakaoka, K. Takanabe and K. Aika, Chem. Commun. 9 (2002) 1006.
[13] N.N. Madikizela and N.J. Coville, J. Mol. Catal. A-Chem. 181 (2002) 129.
[14] N.J. Coville and J.L. Li, Catal. Today 71 (2002) 403.
[15] J.L. Li, L.G. Xu, R. Keogh and B. Davis, Catal. Lett. 70 (2000) 127.
[16] D.G. Wei, J.G. Goodwin Jr., R. Oukaci and A.H. Singleton, Appl. Catal. A 210 (2001) 137.
[17] J.L. Li and N.J. Coville, Appl. Catal. A 208 (2001) 177.
[18] R. Zennaro, M. Tagliabue and C.H. Bartholomew, Catal. Today 58 (2000) 309.
[19] R. Riva, H. Miessner, R. Vitali and G. Del Piero, Appl. Catal. A 196 (2000) 111.
[20] J.L. Li and N.J. Coville, Appl. Catal. A 181 (1999) 201.
[21] A. Kogelbauer, J.C. Weber and J.G. Goodwin Jr., Catal. Lett. 34 (1995) 269.
[22] Y. Zhang, D. Wei, S. Hammache and J.G. Goodwin Jr., J. Catal. 188 (1999) 281.
[23] A. Kogelbauer, J.G. Goodwin Jr. and R. Oukaci, J. Catal. 160 (1996) 125.
[24] D. Schanke, S. Vada, E.A. Blekkan, A. Hilmen, A. Hoff and A. Holmen, J. Catal. 156 (1995) 85.
[25] B.A. Sexton, A.E. Hughes and T.W. Turney, J. Catal. 97 (1986) 390.
[26] P. Arnoldy and J.A. Moulijn, J. Catal. 93 (1985) 38.
[27] A.M. Hilmen, D. Schanke and A. Holmen, Catal. Lett. 38 (1996) 143.
[28] B. Brezny and A. Muan, J. Inorg. Nucl. Chem. 31 (1969) 649.
[29] M. Kraum and M. Baerns, Appl. Catal. A 186 (1999) 189.
[30] Y. Brik, M. Kacimi, M. Ziyad and F. Bozon-Verduraz, J. Catal. 202 (2001) 118.

สถาบันวิทยบริการ
จุฬาลงกรณ์มหาวิทยาลัย

Dependence of Crystalline Phases in Titania on Catalytic Properties

during CO Hydrogenation of Co/TiO$_2$ Catalysts

Bunjerd Jongsomjit*, Chitlada Sakdamnuson and Piyasan Praserthdam

Center of Excellent on Catalysis and Catalytic Reaction Engineering

Department of Chemical Engineering, Faculty of Engineering

Chulalongkorn University, Bangkok 10330, Thailand

*To whom correspondence should be addressed.

E-mail: bunjerd.j@chula.ac.th

สถาบันวิทยบริการ
จุฬาลงกรณ์มหาวิทยาลัย

Abstract

The present research showed dependence of crystalline phases in titania on the catalytic properties of Co/TiO$_2$ catalysts during CO hydrogenation. A comparative study of anatase TiO$_2$- and rultile-anatase coupled TiO$_2$-supported Co catalysts was conducted. It was found that the presence of rutile phase (19 mole%) in tiania resulted in a significant increase in the catalytic activity during CO hydrogenation. It was proposed that the role of rutile phase was to increase the stability of the support. The impact of water vapor produced during reduction on the formation of cobalt species strongly interacted with the support was probably inhibited by the presence of rutile phase in titania leading to a decrease in the reducibility loss during reduction.

สถาบันวิทยบริการ
จุฬาลงกรณ์มหาวิทยาลัย

1. Introduction

In Fischer-Tropsch (FT) catalysis, supported cobalt (Co) catalysts are preferred because of their high activities during FT synthesis based on natural gas [1], high selectivity to linear long chain hydrocarbons and also low activities for the competitive water-gas shift (WGS) reaction [2,3]. Many inorganic supports such as SiO_2 [4-8], Al_2O_3 [9-14], TiO_2 [15-17] and Zeolites [18] have been extensively studied for supported Co catalysts for years. It is known that in general, the catalytic properties depend on reaction conditions, catalyst compositions, metal dispersion, and types of inorganic supports used. Thus, changes the catalyst compositions and/or even though the compositions of supports used may lead to significantly enhance the catalytic properties as well.

During the past decade, titania-supported Co catalysts have been widely investigated by many authors, especially for the application of FT synthesis in a continuously stirred tank reactor (CSTR) [15-17]. However, it should be noted that titania itself has different crystalline phases such as anatase and rutile phases. The different crystalline phase compositions of titania could play an important role on the catalytic performance of titania-supported Co catalysts during CO hydrogenation as well. Thus, the main objective of this research was to investigate influences of different crystalline phases of titania supports on the catalytic properties during CO hydrogenation of Co/TiO_2 catalysts. In the present study, the Co/TiO_2 catalysts were prepared using different crystalline phase compositions of titania supports. The catalysts were pretreated, characterized and tested in order to evaluate the catalytic properties during CO hydrogenation.

2. Experimental

2.1 Catalyst preparation

A 20 wt% of Co/TiO$_2$ was prepared by the incipient wetness impregnation. A designed amount of cobalt nitrate [Co(NO$_3$)•6H$_2$O] was dissolved in deionized water and then impregnated onto TiO$_2$ (contained 100 mole% of anatase phase calcined at 600°C, obtained from Ishihara Sangyo, Japan) and onto TiO$_2$ (contained 81 mole% of anatase phase and 19 mole% of rutile phase, also obtained from Ishihara Sangyo, Japan). The catalyst precursor was dried at 110°C for 12 h and calcined in air at 500°C for 4 h.

2.2 Catalyst pretreatments

2.2.1 Standard reduction

Standard reduction of the calcined catalyst was conducted in a fixed-bed flow reactor under differential conditions at 1 atm using a temperature ramp from ambient to 350°C at 1°C/min and holding at 350°C for 10 h in a gas flow having a space velocity of 16,000 h^{-1} and consisting of H$_2$. The high space velocity of the H$_2$ flow was applied to insure that the partial pressure of water vapor in the catalyst bed produced by cobalt oxide reduction would be essentially zero. The reduced catalyst was then passivated at room temperature with air for 30 min prior to taking it out.

2.2.2 Hydrothermal treatment

4

In order to evaluate the stability of catalysts and impacts of water vapor during reduction, hydrothermal treatment was also conducted during standard reduction above. In addition, besides using pure H_2, mixtures of H_2 and water vapor (5-10 vol%) were also applied separately at the same reduction condition as mentioned in 2.2.1.

2.3 Catalyst nomenclature

The nomenclature used for the catalyst samples in this study is following:

- **Co/T1:** titania (100 mole% of anatase phase)-supported Co catalyst

- **Co/T2:** titania [81 mole% of anatase phase and 19 mole% of rutile phase)-supported Co catalyst

- **(C):** calcined catalyst sample

- **(RW0), (RW5) and (RW10):** reduced catalyst samples with no water vapor, 5 vol% of water vapor, and 10 vol% of water vapor, added during standard reduction, respectively.

2.4 Catalyst characterization

2.4.1 BET surface area: BET surface area of the samples after various pretreatments was performed to determine if the total surface area changes upon the various pretreatment conditions. It was determined using N_2 adsorption at 77 K in a Micromeritics ASAP 2010.

2.4.2 X-ray diffraction: XRD was performed to determine the bulk crystalline phases of catalyst following different pretreatment conditions. It was conducted using a SIEMENS D-5000 X-ray diffractometer with CuK_α (λ =

1.54439 Å). The spectra were scanned at a rate of 2.4 degree/min in the range $2\theta = 20\text{-}80$ degrees.

2.4.3 Scanning electron microscopy and energy dispersive X-ray spectroscopy: SEM and EDX were used to determine the catalyst morphologies and elemental distribution throughout the catalyst granules, respectively. The SEM of JEOL mode JSM-5800LV was applied. EDX was performed using Link Isis series 300 program.

2.4.4 Raman spectroscopy: The Raman spectra of the samples were collected by projecting a continuous wave laser of argon ion (Ar^+) green (514.532 nm) through the samples exposed to air at room temperature. A scanning range of 100 to 1000 cm^{-1} with a resolution of 2 cm^{-1} was applied. The data were analyzed using the Renishaw WiRE (Windows-based Raman Environment) software, which allows Raman spectra to be captured, calibrated, and analyzed using system 2000 functionality via Galactic GRAMS interface with global imaging capacity.

2.4.5 Temperature-programmed reduction: TPR was used to determine the reduction behaviors and reducibilities of the samples. It was carried out using 50 mg of a sample and a temperature ramp from 35 to 800°C at 5°C/min. The carrier gas was 5% H_2 in Ar. A cold trap was placed before the detector to remove water produced during the reaction. A thermal conductivity detector (TCD) was used to determine the amount of H_2 consumed during TPR. The H_2 consumption was calibrated using TPR of Ag_2O at the same conditions.

6

The reduced samples were recalcined at the original calcination conditions prior to performing TPR. The calculation of reducibilities was described in elsewhere [9, 19-22].

2.5 Reaction

CO hydrogenation ($H_2/CO = 10/1$) was performed to determine the overall activity of the catalyst samples reduced at various conditions. Hydrogenation of CO was carried out at $220^{\circ}C$ and 1 atm. A flow rate of $H_2/CO/He = 20/2/8$ cc/min in a fixed-bed flow reactor under differential conditions was used. A relatively high H_2/CO ratio was used to minimize deactivation due to carbon deposition during reaction. Typically, 20 mg of a catalyst sample was re-reduced *in situ* in flowing H_2 (30 cc/min) at $350^{\circ}C$ for 10 h prior to the reaction. Reactor effluent samples were taken at 1 h intervals and analyzed by GC. In all cases, steady-state was reached within 5 h.

3. Results and discussion

The present study was conducted in order to investigate the dependence of crystalline phases in titania on the catalytic properties during CO hydrogenation of Co/TiO_2 catalysts. As mentioned, in general titania used contains mainly two phases; anatase and rutile phases. Phase transformation of titania depends on the preparation of titania such as sol-gel or solvothermal methods and also calcination temperatures. However, it was proposed that the different phase compositions in titania could play an important role on the catalytic properties during CO hydrogenation of Co/TiO_2 catalysts. Results and discussion are divided into two parts as follows:

7

3.1 Catalyst stability during reduction under hydrothermal treatments

It is known that Co metal rather than its oxide or carbide is the active form of supported Co catalysts during CO hydrogenation. Thus, reduction of Co oxide precursor is required in order to reduce it into Co metal form. Water vapor is a byproduct of reduction of metal oxide. It is also known that water vapor also has impacts on the reduction of alumina-supported Co oxide probably in two ways; (i) facilitation of the migration of Co ions into tetrahedral sites of alumina to form a non-reducible (at temperatures < 900°C) spinel and (ii) inhibition of well-dispersed CoO interacting with the alumina support, posssibly by increasing the cobalt-alumina interaction [22]. Moreover, Co-Support compound formation (Co-SCF) can be formed during reduction, especially, when alumina [19] and silica [21] are used as the supports for Co catalysts. Thus, in order to evaluate the impacts of water vapor on the stability of Co/TiO_2 catalysts, hydrothermal treatments during reduction of the catalysts was also performed. After various pretreatments, the catalysts were characterized using different techniques. XRD patterns of samples are shown in **Figure 1**. It can be observed that the T1 support contained pure anatase TiO_2 whereas the T2 support is composed of rutile (19 mole%) and anatase (81 mole%) forms. XRD patterns of T1 showed strong diffraction peaks at 26°, 37°, 48°, 55°, 62°, 69°, 71° and 75° indicating the TiO_2 in its anatase form. The additional diffraction peaks at 27°, 36°, 42° and 57° can been seen in XRD patterns of the T2 support indicating the presence of rutile phase in titania. The cobalt species on both supports exhibited the similar XRD patterns regardless of the pretreatment conditions. As expected, Co_3O_4 were detected at 36°, 46° and 65° after calcination of samples. However, after reduction and passivation, only diffraction peaks at 37° and 63° corresponding to CoO were

8

observed. Raman spectra of all pretreated samples are shown in **Figure 2**. The similar trend in Raman spectroscopy was also observed as seen for XRD results. It was found that T1 support exhibited Raman bands at 640, 514 and 397 cm^{-1} for TiO_2 in its anatase form. Besides the identical Raman bands as shown for the T1 support, the T2 support additionally exhibited a shoulder band around 445 cm^{-1} indicating TiO_2 in its rutile form. The Raman spectra for calcined samples in both T1 and T2 supports exhibited similar Raman bands at 640, 514 and 397 cm^{-1} as seen in those for T1 and T2 supports solely including two shoulders at 690 and 480 cm^{-1}, assigned to Co_3O_4 [9,19, 20]. Raman spectra of all reduced samples showed the Raman bands of titania (T1 or T2) and the shoulders at 690 and 480 cm^{-1}. These can be assigned to Co_3O_4 present on catalyst surface rather than CoO (detected in the bulk by XRD) since Raman spectroscopy is more of surface technique [20]. SEM and EDX were also performed in order to study the morphologies and elemental distributions of catalyst after various pretreatments. However, no significant changes in morphologies and elemental distributions (not shown) were observed upon various pretreatment conditions used in this study. In summary, it should be noted that upon the various pretreatments even with or without hydrothermal treatments, the cobalt species on both T1 and T2 supports, essentially, exhibited the similar characteristics detected by XRD, Raman spectroscopy, and SEM/EDX. No surface compound species between Co and titania, if present, can be detected using those above techniques.

TPR was performed to study reduction behaviors and to measure reducibility of catalysts. TPR profiles of all samples and Co_3O_4 are shown in **Figure 3**. It was found that TPR profile of titania supports (not shown) for both T1 and T2 supports exhibited no reduction peak at this TPR condition. Only one strong reduction

peak (max. at 430°C) can be observed for bulk Co_3O_4 assigned to the overlap of two-step reduction of Co_3O_4 to CoO and then to Co^0 [22-24]. Upon the TPR conditions, the two-step reduction may or may not be observed. For T1 support, only one reduction peak located at ca. 370-620°C (max. at 520°C) can be observed for the calcined sample (Co/T1-C) indicated that no residual cobalt nitrates remain on the calcined samples upon calcination condition used in this study. TPR profiles for all reduced samples with T1 support were also similar exhibiting only one reduction peak located at ca. 400-620°C. The maximum temperature at ca. 520°C for Co/T1-RW0 was shifted about 10 and 20°C when hydrothermal treatment was performed during reduction as seen for Co/T1-RW5 and Co/T1-RW10 samples, respectively. The shift of a reduction peak to a higher temperature (ca. 10-20°C) indicates stronger interaction between cobalt and titania support. It is known that the amounts of Co species strongly interacted with the support are also proportional to the partial pressure of water vapor present during reduction [9, 19-22]. For the T2 support, all pretreated samples also exhibited only one reduction peak (max. at 510°C). However, it should be mentioned that there was no significant shift of the reduction temperatures upon the hydrothermal treatment during reduction indicating a lesser degree of cobalt-support interaction compared to what we have seen for the cobalt species on the T1 support. It was suggested that the presence of rutile phase (19 mole%) in T2 should result in an increase in stability of the titania support even though hydrothermal treatment was applied during reduction. An increase in stability of T2 support could be the cause for a difficulty of cobalt to interact with it.

Besides reduction behaviors obtained from TPR results, reducibilities of samples can be measured based on the peak areas, which are related to the

amounts of hydrogen consumed during TPR [9, 19-22]. The calculated reducibilities along with the BET surface areas of samples are shown in **Table 1**. There was no significant change in surface areas upon the pretreatment conditions used in this study. It was observed that for both T1 and T2 supports, the reducibilities decreased when the calcined samples were reduced and performed TPR indicating a loss in reducibility of cobalt oxide species after reduction [25]. The loss in reducibilities can be probably attributed to a non-reducible (at temperatures < 800°C) "Co-titanate" species formed during standard reduction [25]. However, when considering the reducibility loss of the reduced samples without hydrothermal treatment (RW0 samples), it was found that the reducibility loss after reduction for Co/T2-RW0 sample was only 5% whereas the 24% reducibility loss after reduction was observed for Co/T1-RW0 sample. A degree of reducibility loss also increased with the amounts of water vapor added during reduction for both T1 and T2 supports. In order to illustrate the reducibility loss upon the hydrothermal treatment during standard reduction for both T1 and T2 supports, **Figure 4** is also present. This is to provide a better idea how the presence of rutile phase leads to an increase in stability of the catalysts upon reduction and hydrothermal treatments in term of the reducibility loss after reduction under various conditions.

3.2 Catalytic properties

In order to determine the effect of crystalline phases of titania on the catalytic properties of Co/TiO$_2$, CO hydrogenation was also conducted in a fixed-bed flow reactor under differential conditions. Results obtained from the reaction study are shown in **Table 2**. It was found that both initial and steady-state rates increased

significantly upon the presence of rutile phase in titania as seen for catalysts on the T2 support. However, the increased activities for catalysts on the T1 support strongly depended on the pretreatment conditions used. For catalysts on the T1 support, it was shown that decreases in both initial and steady-state activities were proportional to the amounts of water vapors added during standard reduction. It should be also noted that decreases in activities were also related to the loss in reducibilities after standard reduction as well. Considering both initial and steady-state rates for catalysts on the T2 support, the phenomenon was essentially different from those for the T1 support. It was found that activities for catalysts on the T2 support exhibited much higher activities than those on the T1 support, especially, at the same hydrothermal treatment conditions. Moreover, the initial activities of catalysts on the T2 support exhibited a lesser degree of decreased rates until they reached the steady-state rates compared to those on the T1 support. In addition, for catalysts on the T2 support, both initial and steady-state rates showed consistency in rates regardless of the pretreatment conditions used indicating high stability of catalysts. This is suggested that the hydrothermal treatment conditions used have no effect on the catalytic activities during CO hydrogenation of catalysts on the T2 support. This can be explained by the increased stability of T2 support due to the presence of rutile phase in titania resulting in an inhibition of Co-support compound formation (Co-SCF) [19,20] in the titania support [25].

Since the surface areas of the T1 (70 m^2/g) and T2 (49 m^2/g) supports were slightly different, one might think that a change in surface areas of the supports probably has the effect on rates as well. In order to elucidate this doubt, reaction study was also conducted using titania supports (anatase form only) with various

surface areas. Results obtained from the reaction study are shown in **Table 3**. It was found that basically, both initial and steady-state activities increased with increasing surface areas from 70 to 170 m^2/g for catalysts on pure anatase titania. This should be due to higher Co dispersion in larger surface areas of supports leading to an increase in the number of reduced surface Co metal atoms available for catalyzing the reaction. Thus, if one considered the dependence of rates based on the surface areas solely, catalysts on the T2 support, which had smaller surface areas would result in lower activities due to a decreased surface area. However, it is not true for what we have found in this present study. Essentially, even though the surface area of the T2 support was only 49 m^2/g, which was smaller than that for the pure anatase titania, activities of catalysts on the T2 support were still exceptional high with the presence of rutile phase in titania. This indicated that the presence of rutile phase in titania can result in an enhancement of catalytic activities of Co/TiO$_2$ catalyst during CO hydrogenation. Increases in activities were probably due to; (i) high stability to the hydrothermal treatment of the support used and (ii) the presence of a higher number of reduced Co metal atoms resulted from the lesser amounts of Co-SCF.

Considering the selectivity of products during methanation, which is also shown in **Table 2**. It was found that catalysts on the T2 support exhibited higher selectivity to methane compared to those on the T1 support. This was suggested that catalysts on the T1 support produced more long chain hydrocarbons than those on the T2 support. This indicated that the presence of rutile phase on titania probably resulted in a lesser amounts of long chain hydrocarbons. In general, it has been known that catalytic activities of supported Co catalyst depend only on the number of surface reduced cobalt atoms available for catalyzing the reaction.

Mostly, changes in catalytic activities do not alter the selectivity of products since only the number of active sites change, but the nature of active sites would be the same. However, in this case, we found a slight change in product selectivity. This indicated that the presence of rutile phase in titania affected not only on activities of Co/TiO_2 catalysts, but perhaps also on the selectivity of products as well. In order to give the best answer for how the presence of rutile phase affects the selectivity of products during CO hydrogenation, a rigorous study should be further investigated in more details. It is recommended that techniques such as steady-state isotropic transient kinetic analysis (SSITKA) or other surface analysis techniques must be applied in order to provide more details on the surface intermediates. Thus, this is not the main focus of our present study at this time. Besides, influences of rutile phase in titania on product distributions, an investigation of how the mole ratios of rutile per anatase phase affect the catalytic properties will be our main focus in the near future.

4. Conclusions

The present study has shown the dependence of crystalline phases in titania on the catalytic properties during CO hydrogenation of Co/TiO_2 catalysts. The presence of rutile phase (19 mole%) in titania resulted in significant increases in the catalytic activities during CO hydrogenation. This is mostly due to an increase in stability of the titania support with the presence of rutile phase. It was found that the presence of rutile phase enhanced the stability of the titania support and also catalysts themselves leading to lesser degrees of a loss in reducibility after hydrothermal treatments during reduction of catalysts. It was proposed that the presence of rutile phase in titania stabilized the catalysts probably due to two

reasons; (i) block the formation of Co species strongly interacted with the titania support or Co-SCF and (ii) inhibition of the impact of water vapor produced during reduction.

Acknowledgements

References

1. Wither, Jr., H.P., Eliezer, K.F., and Mechell, J.W., *Ind. Eng. Chem. Res.* **29**, 1807 (1990).

2. Iglesia, E., *Appl. Catal. A.* **161**, 59 (1997).

3. Brady, R.C., and Pettie, R.J., *J. Am. Chem. Soc.* **103**, 1287 (1981).

4. Martinez, A., Lopez C., Marquez, F., and Duaz, I., *J. Catal.* **220**, 486 (2003).

5. Panpranot, P., Goodwin, Jr., J.G., and Sayari, A., *Catal. Today* **77**, 269 (2002).

6. Panpranot, P., Goodwin, Jr., J.G., and Sayari, A., *J. Catal.* **211**, 530 (2002).

7. Sun, S.L., Isubaki, and Fujimoto, K., *Appl. Catal. A.* **202**, 121 (2000).

8. Ali, S., Chen B., and Goodwin, Jr., J.G., *J. Catal.* **157**, 35 (1995).

9. Jongsomjit, B., Panpranot, J., and Goodwin, Jr., J.G., *J. Catal.* **215**, 66 (2003).

10. Das, T., Jacobs, G., Patterson, P.M., Conner, W.A., Li, J.L., and Davis, B.H., *Fuel* **82**, 805 (2003).

11. Jacobs, G., Patterson, P.M., Zhang, Y.Q., Das, T., Li, J.L., and Davis B.H., *Appl. Catal. A.* **233**, 215 (2002).

12. Rothaemel, M., Hanssen, K.F., Blekkan, E.A., Schanke, D., and Holmen, A., *Catal. Today* **38**, 79 (1997).

13. Ragai V., Carli, R., Bianchi, C.L., Lorenzetti, D., and Vergani, G., *Appl. Catal. A.* **139**, 17 (1996).

14. Ragaini V., Carli, R., Bianchi, C.L., Lorenzetti, D., Predieri, G., Moggi, P., *Appl. Catal. A.* **139**, 31 (1996).

15. Li, J.L., Jacobs, G., Das, T., and Davis, B.H., *Appl. Catal. A.* **233**, 255 (2002).

16. Jacobs, G., Das, T., Zhang, Y.Q., Li, J.L., Racoillet, G., and Davis, B.H., *Appl. Catal. A.* **233**, 263 (2002).

17. Li, J.L., Xu, L.G., Keogh, R., and Davis, B.H., Catal. Lett. 70, 127 (2000).

18. Li, X.H., Asami, K., Luo, M.F., Michiki, K., Tsubaki, N., and Fujimoto, K., Catal. Today 84, 59 (2003).

19. Jongsomjit, B., Panpranot, J., and Goodwin, Jr., J.G., *J. Catal.* **204**, 98 (2001).

20. Jongsomjit, B., and Goodwin, Jr., J.G., *Catal. Today* **77**, 191 (2002).

21. Kogelbauer, A., Weber, J.C., and Goodwin, Jr., J.G., *Catal. Lett.* **34**, 269 (1995).

22. Zhang, Y., Wei, D., Hammache, S., and Goodwin, Jr., J.G., *J. Catal.* **188**, 281 (1999).

23. Schanke, D., Vada, S., Blekkan, E.A., Hilmen, A., Hoff, A., and Holmen, A., *J. Catal.* **156**, 85 (1995).

24. Sexton, B.A., Hughes, A.E., and Turney, T.W., *J. Catal.* **97**, 390 (1986).

25. Jongsomjit, B., Sakdamnuson, C., Goodwin, Jr., J.G., and Praserthdam, P., *Catal. Lett.* **94**, 209 (2004).

Table 1 Surface areas, reducibilities and reducibility loss after reduction of samples after various pretreatments.

Samples	Surface Area (m^2/g)	Reducibility during TPR at 35-800°C[a,b] (%)	Reducibility Loss after Reduction[c] (%)
T1	70	0	-
T2	49	0	-
Co/T1 (C)	52	92	n/a
Co/T2 (C)	37	78	n/a
Co/T1 (RW0)	49	70	24
Co/T2 (RW0)	37	74	5
Co/T1 (RW5)	46	68	26
Co/T2 (RW5)	37	72	8
Co/T1 (RW10)	46	64	30
Co/T2 (RW10)	36	68	13

[a] The reduced samples were recalcined at the original calcination conditions prior to performing TPR.

[b] Measurement error is ±5%

[c] Reducibility loss (%) after reduction was calculated from
[(Reducibility of calcined sample – Reducibility of reduced sample) x 100/]/
Reducibility of calcined sample

Table 2 Reaction study during CO hydrogenation of catalyst samples pretreated under various conditions.

Samples	CO Conversion[a] (%)		Rate[b] ($\times 10^2$ gCH$_2$/gcat.h)		CH$_4$ Selectivity (%)	
	Initial[c]	SS[d]	Initial	SS	Initial	SS
Co/T1 (C)	3.7	2.1	1.4	0.8	71	68
Co/T2 (C)	67.4	54.9	25	21	94	96
Co/T1 (RW0)	1.5	0.7	0.6	0.3	68	65
Co/T2 (RW0)	60.8	53.1	23	20	94	94
Co/T1 (RW5)	0.8	0.5	0.3	0.2	71	70
Co/T2 (RW5)	60.6	52.8	23	20	98	98
Co/T1 (RW10)	0.3	0.1	0.1	0.03	73	69
Co/T2 (RW10)	60.2	52.6	23	19	95	96

[a]CO hydrogenation was carried out at 220°C, 1 atm and H$_2$/CO/He = 20/2/8 cc/min

[b]Error ±5%

[c]After 5 min of reaction

[d]after 5 h of reaction

สถาบันวิทยบริการ
จุฬาลงกรณ์มหาวิทยาลัย

Table 3 Influence of surface area of TiO_2 on catalytic properties of supported cobalt catalysts during CO hydrogenation.

Samples	Surface Area (m^2/g)	CO Conversion[c] (%)		Rate[f] (10^2 gCH$_2$/gcat.h)	
		Initial[d]	SS[e]	Initial	SS
Co/T1 (C)	70	3.7	2.1	1.4	0.8
Co/T3[a] (C)	145	42.7	9.4	16	4
Co/T4[b] (C)	170	59.6	12.2	22	4
Co/T2 (C)	49	67.4	54.9	25	21

[a]T3 is TiO_2 (pure anatase) which has surface area of 145 m^2/g

[b]T4 is TiO_2 (pure anatase) which has surface area of 170 m^2/g

[c]CO hydrogenation was carried out at 220^oC, 1 atm and H_2/CO/He = 20/2/8 cc/min

[d]After 5 min of reaction

[e]After 5 h of reaction

[f]Error $\pm 5\%$
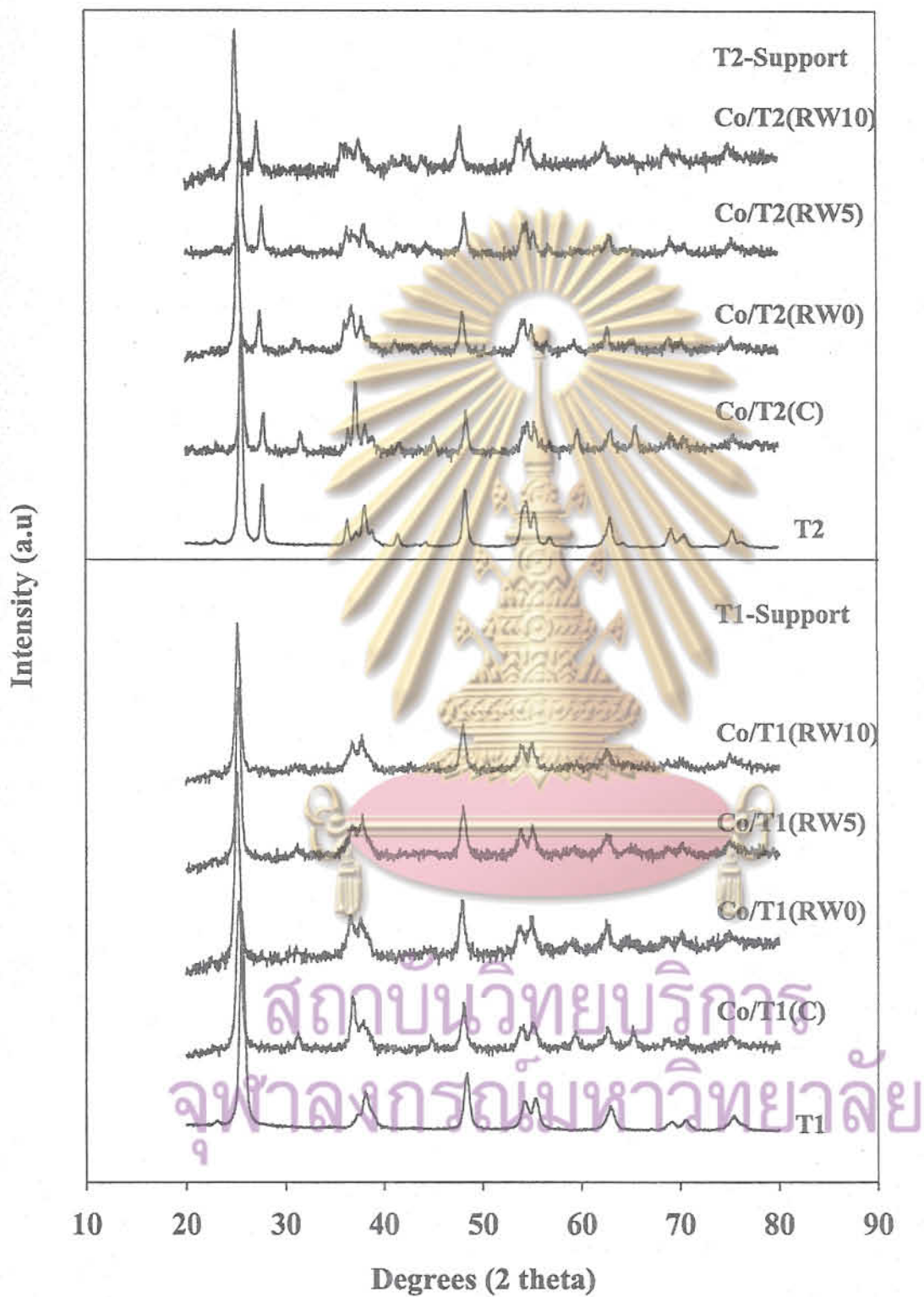
สถาบันวิทยบริการ
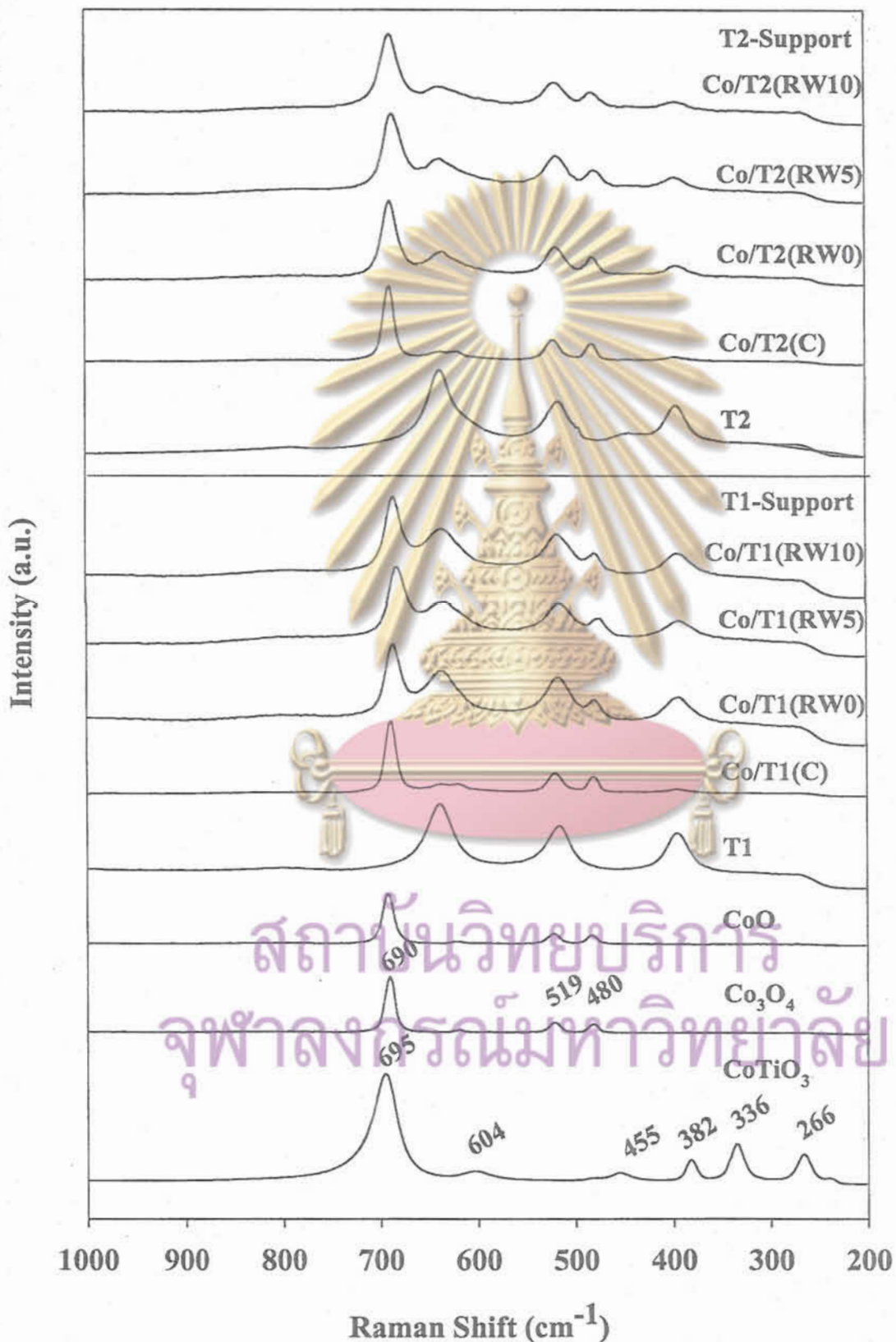จุฬาลงกรณ์มหาวิทยาลัย

List of Figures
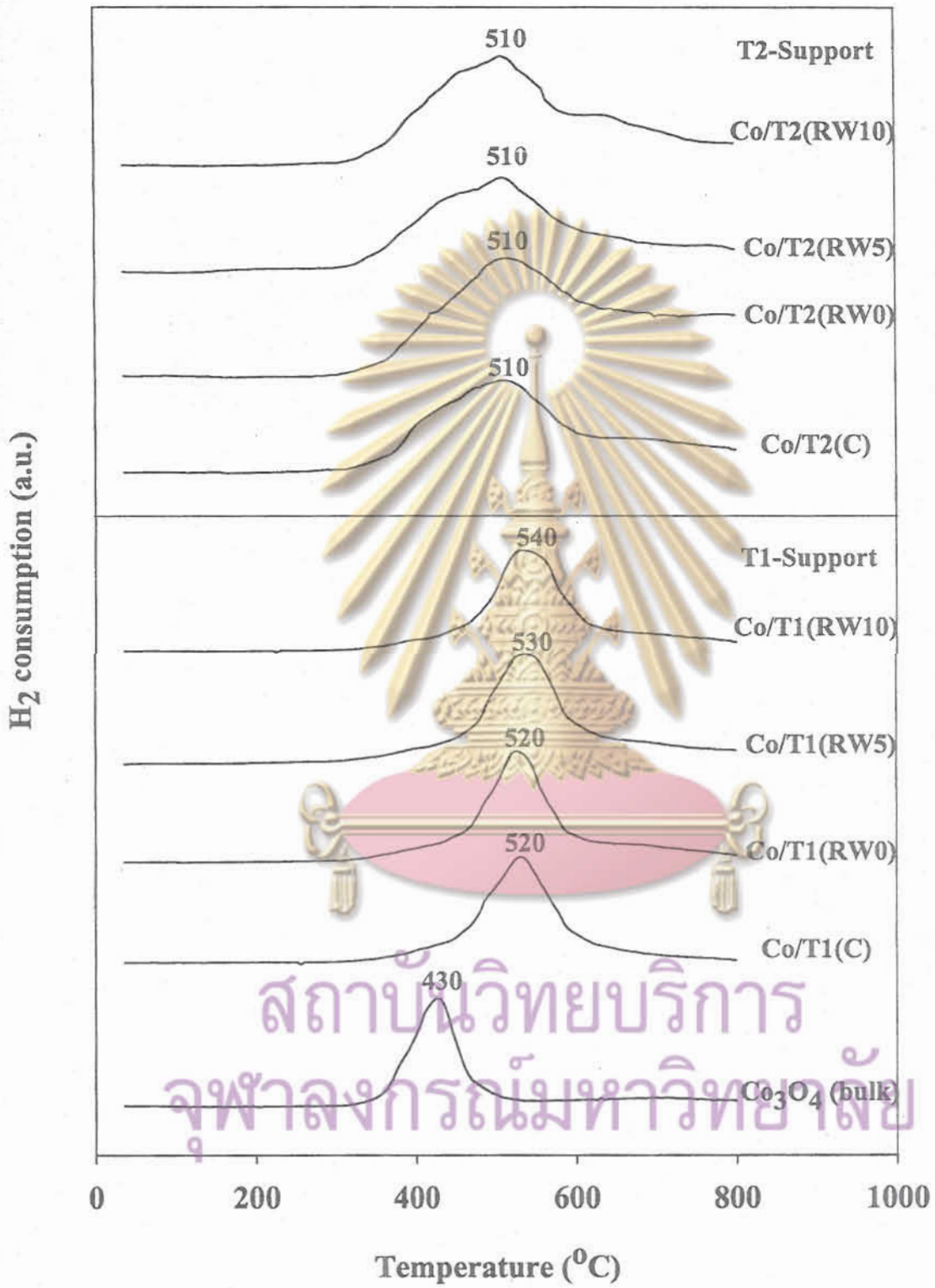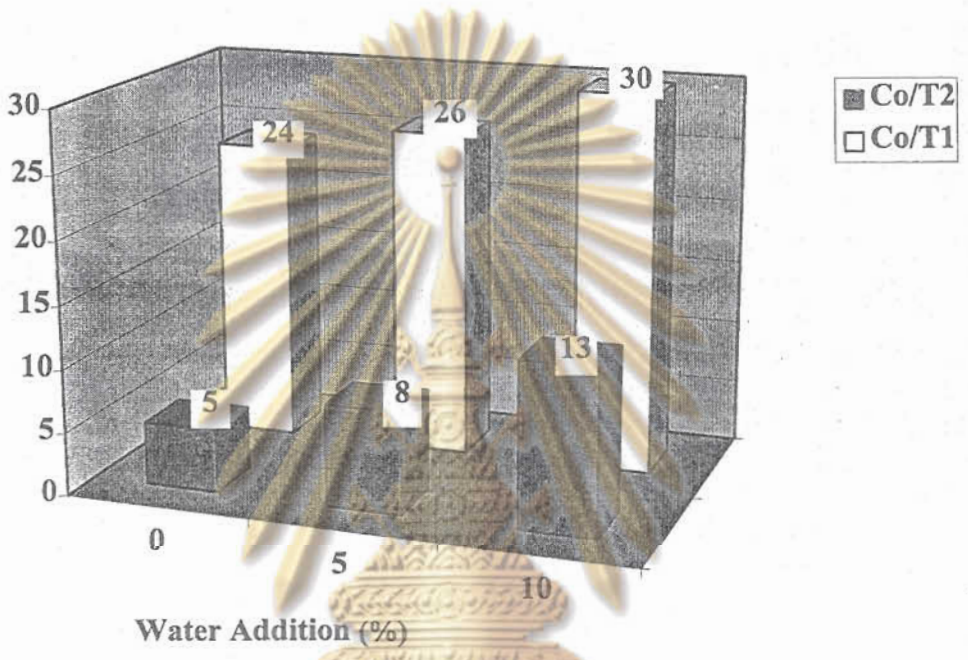
Figure 1

Figure 2

Figure 3

23

Figure 4

สถาบันวิทยบริการ
จุฬาลงกรณ์มหาวิทยาลัย

METAL-SUPPORT INTERACTION IN MESOPOROUS SILICA SUPPORTED COBALT FISCHER-TROPSCH CATALYSTS

Joongjai Panpranot[*], Sujaree Kaewgun, and Piyasan Praserthdam

Center of Excellence on Catalysis and Catalytic Reaction Engineering, Department of Chemical Engineering, Chulalongkorn University, Bangkok, Thailand

* To whom correspondence should be addressed.

Tel: (66)-2-218-6859, Fax: (66)-2-218-6877, Email: joongjai.p@eng.chula.ac.th
ABSTARCT

The metal-support interaction in silica supported Co Fischer-Tropsch catalysts does not depend on the pore structure of the support (SiO_2 or MCM-41) but is primarily affected by the metal particle size.

INTRODUCTION

Cobalt-based catalysts are widely used in CO hydrogenation or Fischer-Tropsch synthesis (FTS) especially when high molecular weight paraffins are preferred [1-2]. To increase their activity, cobalt is usually deposited on a high surface area oxide support to obtain a high metal dispersion. Recently, the use of high surface area ordered mesoporous materials such as MCM-41 and SBA-15 for preparing Co-based Fischer-Tropsch catalysts has been explored [3-7]. Compared to amorphous silica-supported catalysts with similar Co loading, Co supported on these mesoporous materials have shown higher FTS activity due to a better dispersion of cobalt in mesoporous structure [8]. However, stronger interaction of cobalt species and the support in these catalysts were often found, resulted in catalysts with lower reducibilities. In this study, the effects of pore structure (SiO_2 and MCM-41) and the metal particle size on the metal-support interaction in supported Co F-T catalysts were investigated.

EXPERIMENTAL

Catalyst Preparation

Pure silica MCM-41 was prepared in the same manner as that of Kruk et al. [9] using the following gel composition: (1.0 SiO_2): (0.317 TMAOH): (0.45 CTMABr): (66.7 H_2O), where TMAOH denotes tetramethylammonium hydroxide and CTMABr denotes cetyltrimethyl ammonium bromide. High surface area SiO_2 with similar pore size to MCM-41 were obtained from Grace Davison Company. The series of supported Co catalysts (MCM-41 and SiO_2-supported) were prepared by the incipient wetness impregnation of the supports with an aqueous solution containing the desired amount of different cobalt precursors such as cobalt nitrate (Aldrich), cobalt acetate (APS), cobalt acetylacetonate (Aldrich), and cobalt chloride (Fluka). The elemental analysis for all the catalysts gave cobalt loading ca. 8 wt%. The catalysts were dried overnight in an oven at 110°C and then were calcined at 500°C in an air flow for 2 h.

Catalyst characterization

The BET surface area, pore volume, average pore diameter, and pore size distribution of the catalysts were determined by N_2 physisorption using a Micromeritics ASAP 2000 automated system. Each sample was degassed in the Micromeritics ASAP 2000 at 150°C for 4 h prior to N_2 physisorption. The XRD spectra of the catalysts were measured using a SIEMENS D5000 X-ray diffractometer, using Cu Kα radiation with a Ni filter in the 2-8° or 10-80°2θ angular regions. Temperature programmed reduction was performed using an in-house system and a temperature ramp of 5°C/min from 30 to 300°C in a flow of 5% H_2 in argon. Approximately 0.20 g of a calcined catalyst was placed in a

quartz tube in a temperature-controlled oven and connected to a thermal conductivity detector. The H_2 consumption was measured by analyzing the effluent gas with a TCD.

Reaction study

CO hydrogenation was carried out at 220°C and 1 atm total pressure in a fixed-bed stainless steel reactor under differential conversion conditions. A flow rate of $H_2/CO/Ar = 20/2/8$ cm^3/min was used. Typically, 0.2 g of the catalyst samples was reduced *in situ* in flowing H_2 (50 cc/min) at 350°C for 10 h prior to reaction. The product samples were taken at 1-h intervals and analyzed by gas chromatography. Steady state was reached after 6 h time-on-stream in all cases.

RESULTS AND DISCUSSION

In order to distinguish the effect of pore size and pore structure of the supports, high surface area SiO2 and MCM-41 with the same average pore diameter were employed as a support for preparation of the catalysts. The BET surface areas, pore volumes, and average pore diameters of the original supports and the catalysts are given in Table 1. The significant decrease in surface area of the original support material suggests that cobalt was deposited in some of the pores of the supports. The XRD patterns of SiO_2 and MCM-41 supported Co catalysts after calcinations in air at 500°C for 2 h (Figure 2) were quite similar where only the catalysts prepared from cobalt nitrate and cobalt chloride exhibited the diffraction peaks of Co_3O_4. This suggested that the cobalt oxide particle sizes

obtained from organic precursors were much smaller than those prepared form inorganic ones [10].

The temperature program reduction (TPR) profiles of SiO_2- and MCM-41-supported Co catalysts are shown in Figure 3. In general, two-step reduction can be observed; reduction of Co_3O_4 to CoO and then CoO to Co^0 [11-12]. In this study, TPR profiles of high surface area silica supported Co catalysts were affected strongly by the cobalt precursors. Using organic cobalt precursors such as cobalt acetate and cobalt acetylacetonate which could result in very small cobalt particles and stronger metal-support interaction showed much higher reduction temperature. Any Co not reducible during the H_2 reduction up to 800°C is identified as "non-reducible" Co silicate [13-14]. Similar TPR profiles were observed on SiO_2 and MCM-41 supported Co catalysts prepared with the same Co precursor suggesting that there was less impact of the pore structure of the support on metal-support interaction on the catalysts.

The results of CO hydrogenation reaction test are reported in Table 2. It was found that Co-/M-NO exhibited the highest CO hydrogenation rate than all other catalysts in this study. The higher activity of such catalyst was probably due to their higher dispersion of cobalt (higher pore volume and BET surface area). The catalysts prepared from cobalt chloride showed very low activities due to their low Co dispersion and maybe residual Cl⁻ blocking Co active sites [10]. The low activities of the ones prepared from cobalt acetate and cobalt acetyl acetonate were due probably to the unstable small Co particles forming Co silicates during reduction in H_2 and reaction.

References

1 R. B. Anderson, "The Fischer-Tropsch Synthesis", Academic Press, San Diego, 1984.

2 J. G. Goodwin, Jr.: *Prep.ACS Div. Petr. Chem.*, **36**, 156 (1991).

3 D. Yin, W. Li, W. Yang, H. Xiang, Y. Sun, B. Zhong, S. Peng: Micropor. Mesopor. Mater., **47**, 15 (2001).

4 J. Panpranot, J. G. Goodwin, Jr., A. Sayari: *Catal. Today*, **77**, 269 (2002).

5 Y. Wang, M. Noguchi, Y. Takahashi, Y. Ohtsuka: *Catal. Today*, **68**, 3 (2001).

6 A. Y. Khodakov, A. Griboval-Constant, R. Bechara, V. L. Zholobenko: *J. Catal.*, **206**, 230 (2002).

7 A. Martinez, C. Lopez, F. Marquez, and I. Diaz: *J. Catal.*, **220**, 486 (2003).

8 J. Panpranot, J. G. Goodwin, Jr., and A. Sayari: *J. Catal.*, **211**, 530 (2002).

9 M. Kruk, M. Jaronice, and A. Sayari: *Microporous and Mesoporous Mater.*, **35-36**, 545 (2000).

10 J. Panpranot, S. Kaewgun, P. Praserthdam, and J. G. Goodwin, Jr.: *Catal. Lett.*, **91**, 95 (2003).

11 A.M. Hilmen, D. Schanke, and A. Holmen: Catal .Lett., **38**, 143 (1996).

12 Y. Zhang, D. Wei, S. Hammache, and J.G. Goodwin, Jr.: *J. Catal.*, **188**, 281 (1999).

13 A. Kogelbauer, J. C. Weber, and J.G. Goodwin, Jr.: *Catal. Lett.*, **34**, 259 (1995).

14 J. M. Jablonski, M. Wolcyrz, and L. Krajczyk: *J. Catal.*, **173**, 530 (1998).

สถาบันวิทยบริการ
จุฬาลงกรณ์มหาวิทยาลัย

Table 1: The Characteristics of SiO_2 and MCM-41 Supported Co Catalysts.

Catalyst	Co (wt%)	BET S.A. (m^2/g)	dp Co_3O_4 (nm)
SiO_2	-	717	-
Co/S-Ac	7.9	562	n/a
Co/S-AA	7.7	595	n/a
Co/S-Cl	7.1	517	17.6
Co/S-NO	8.4	571	16.4
MCM-41	-	1234	-
Co/M-Ac	8.3	756	n/a
Co/M-AA	7.8	675	n/a
Co/M-Cl	7.1	646	15.0
Co/M-NO	8.1	747	6.3
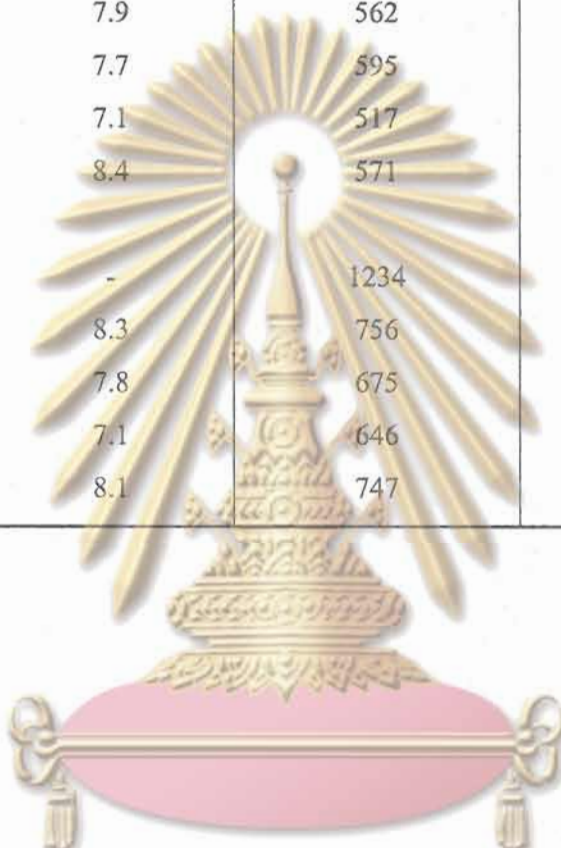
สถาบันวิทยบริการ
จุฬาลงกรณ์มหาวิทยาลัย

Table 2. Results from CO Hydrogenation Reaction[a]

Catalyst	Rate (gCH$_2$/ gcat./h)		CO Conversion (%)		Selectivity (%)		
	Initial	Steady-state	Initial	Steady-state	CH$_4$	C$_2$	C$_3$
Co/S-Ac	0.012	0.010	2.1	1.4	95	4.5	0.5
Co/S-AA	0.013	0.012	1.7	1.6	96	3.5	0.5
Co/S-Cl	0.007	0.006	0.9	0.8	84	13.0	3.0
Co/S-NO	0.176	0.167	23.4	22.7	95	5.0	-
Co/M-Ac	0.025	0.018	3.2	2.4	91	7.0	2.0
Co/M-AA	0.013	0.013	1.8	1.7	96	3.4	0.6
Co/M-Cl	0.024	0.018	3.3	2.4	97	2.5	0.5
Co/M-NO	0.449	0.323	59.8	47.6	82	6.0	2.0

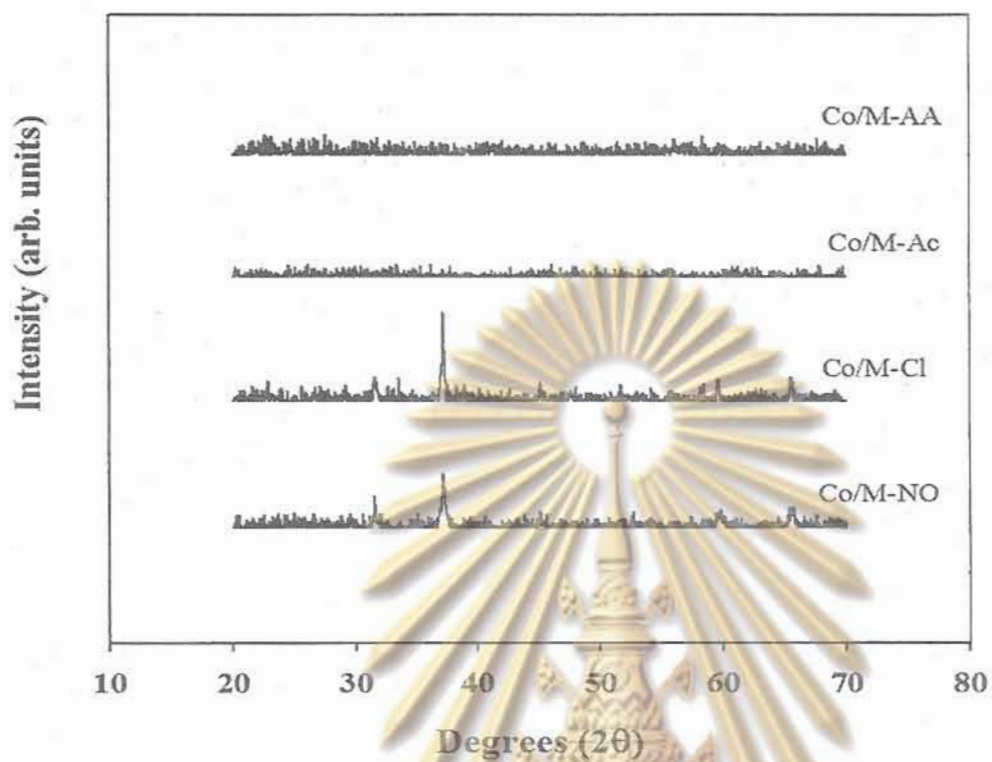[a] Reaction conditions are 220°C, 1 atm, and H$_2$/CO = 10.

Figure 1. XRD patterns of different SiO₂ and MCM-41-supported Co catalysts
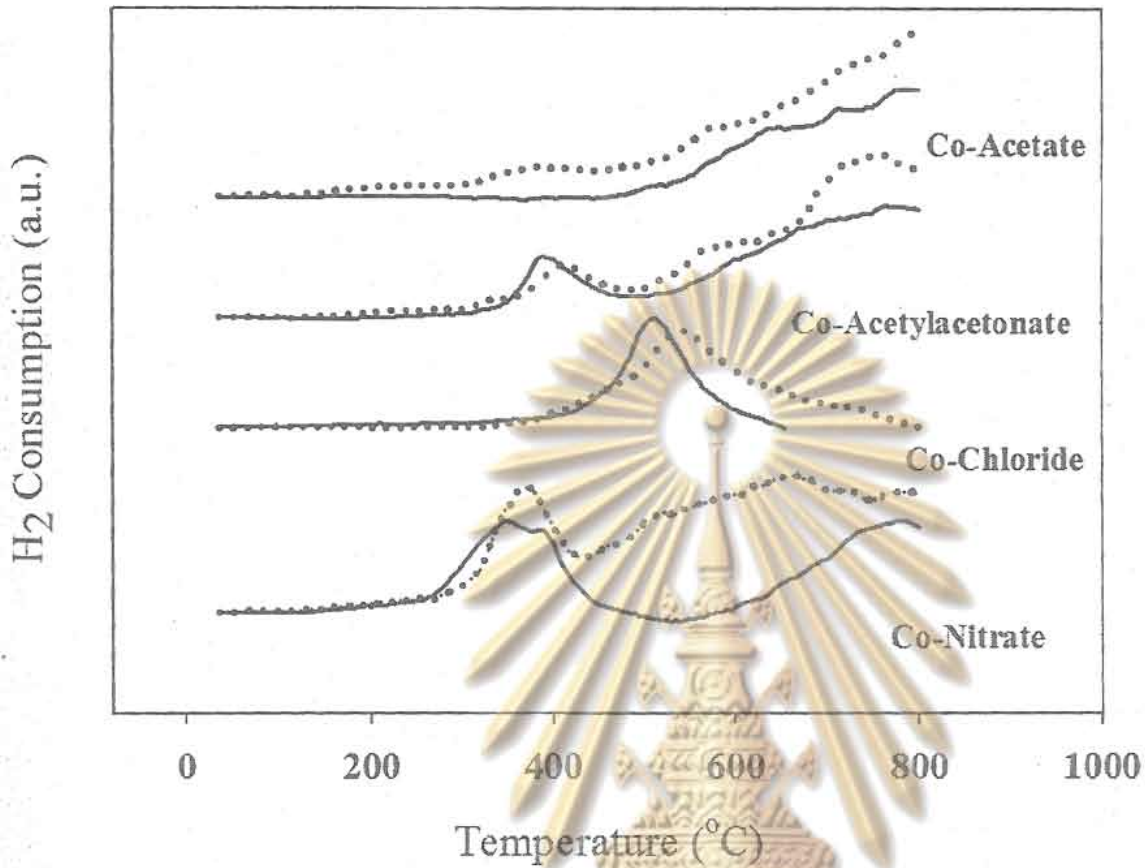
สถาบันวิทยบริการ
จุฬาลงกรณ์มหาวิทยาลัย

Figure 2: Temperature program reduction (TPR) profiles of Co/MCM-41 (·······) and Co/SiO₂ (——).

สถาบันวิทยบริการ
จุฬาลงกรณ์มหาวิทยาลัย